Available online at www.sciencedirect.com
ScienceDirect
Journal of Sound and Vibration 324 (2009) 1039–1066
JOURNAL OF SOUND AND VIBRATION
www.elsevier.com/locate/jsvi

Gaussian orthogonal ensemble spacing statistics and the statistical overlap factor applied to dynamic systems

Nicole J. Kessissoglou*, Geoff I. Lucas

School of Mechanical and Manufacturing Engineering, The University of New South Wales, Sydney, NSW 2052, Australia

Received 30 August 2006; received in revised form 28 October 2008; accepted 7 February 2009
Handling Editor: L.G. Tham
Available online 19 March 2009

Abstract

This paper examines the extent to which Gaussian orthogonal ensemble (GOE) statistics is applicable to the natural frequencies of a dynamic system. The natural frequencies of a simply supported plate or a rectangular room tend to have an exponential spacing distribution. However, any disruption of the system symmetries has been shown to promote GOE statistics, for which the modal spacing distribution is Rayleigh. In this paper, the effect of a range of uncertainties on the modal statistics of structures is numerically characterised. This is achieved by examining the modal statistics of mass and/or spring loaded plates and plates coupled by springs. The natural frequencies of the aforementioned structures have been derived using the Lagrange–Rayleigh–Ritz technique. The degree of uncertainty required to effect the transition from an exponential to a Rayleigh distribution and to achieve universality of the statistical properties is investigated. A further measure of the randomness required to produce GOE statistics can be obtained by examining the amount of mixing and veering between the modes of a dynamic system. The statistical overlap factor is a non-dimensional parameter related to the random variation in an individual natural frequency from its mean value, and is useful to quantify the frequency beyond which the resonant behaviour of individual modes no longer dominates the response statistics. Using a first-order perturbation analysis, an approximate expression for the statistical overlap factor has been developed for the randomised plates, to estimate the modal range for the occurrence of GOE statistics.

1. Introduction

There has been much recent interest in predicting the response of stochastic systems [1–3], since most practical structures exhibit some form of randomness due to variability in their geometric or material properties. Prediction methods for the response of a structure with uncertain properties generally require some model for the statistics of the natural frequencies of the system. Earlier work on the natural frequency statistics of dynamic systems used a Poisson point process model to describe the distribution of the spacing between successive natural frequencies, which results in an exponential distribution of the modal spacing [4]. However, the Poisson model, resulting in an exponential distribution of the modal spacings, is only valid for

*Corresponding author. Tel.: +61 2 9385 4166; fax: +61 2 9663 1222.
E-mail address: n.kessissoglou@unsw.edu.au (N.J. Kessissoglou).

0022-460X/$ - see front matter
doi:10.1016/j.jsv.2009.02.014

systems such as a perfect rectangular plate or a perfect box-shaped room, where these systems have many symmetries [5]. In these examples, it is possible for frequencies from different symmetry groups to coincide, giving a high probability of small modal spacings. Any disturbance of the system will cause coupling of the symmetry groups and veering between closely spaced natural frequencies, leading to a reduced probability of small spacings. It is now thought that the natural frequency statistics of practical structures, with randomness in their geometric or material properties, will conform to those associated with a particular type of random matrix known as the Gaussian orthogonal ensemble (GOE), and this assumption has been adopted in recent response prediction methods [5–8]. One feature of the GOE is that the distribution of spacings between successive natural frequencies is Rayleigh, rather than exponential, and this constitutes the "Wigner surmise" of random matrix theory [5].

The transition from an exponential to a Rayleigh distribution for a *single* dynamic system has been experimentally and empirically validated by several authors, by deforming the geometry of rectangular blocks [6–8]. The effect of symmetry breaking on the distribution of the frequency spacings was examined by cutting slits into aluminium blocks [6], deforming the rectangular boundaries to a Sinai billiard shape [7], and by adding mass and stiffness perturbations to steel plates [8,9]. Uncertainty also applies to the response statistics of an *ensemble* of nominally identical structures such as successive items from a production line, where uncertainties arise from the assembly process and manufacturing tolerances [1,10]. In this case, the natural frequencies and modes shapes of a system can be thought of as being random across the ensemble. A measure of the randomness across the ensemble required to produce GOE statistics can be obtained using a non-dimensional parameter called the statistical overlap factor, S [11]. Statistical overlap occurs when there is sufficient random variation in an individual natural frequency of a system from its mean value across the ensemble. Low values of the statistical overlap factor imply that the natural frequencies are in well defined positions and move by only a small amount from their mean value. As S increases, the natural frequencies move significantly and may veer from one another. In this case, there will be good 'mixing' of the modes of the perfect structure across the ensemble, that is, a particular mode shape of a given structure has contributions from a number of the modes of the nominally perfect system [10].

This paper numerically characterises the effect of a range of structural uncertainties on the modal statistics of dynamic structures, and the degree of uncertainty required to achieve universality of the statistical properties. The work of Brown [9] has been extended to investigate the modal statistics of complex systems with a range of uncertainty, corresponding to uncertainty due to mass and stiffness perturbations, uncertainty at the boundaries of a structure and uncertainty in the coupling between structures. A range of structures are examined corresponding to a plate with masses and/or linear springs added at random locations, a plate with torsional springs attached at random locations along its boundary edges and two plates coupled by linear springs at random locations. For the aforementioned structures, equations of motion in modal space were developed using the Lagrange–Rayleigh–Ritz technique. Dynamic uncertainty across an ensemble of nominally identical structures is also investigated using a non-dimensional parameter called the statistical overlap factor. Based on a first-order perturbation analysis and using Rayleigh's quotient, an approximate expression for S was developed for the mass and spring loaded plates. By varying the size and number of the added masses and springs, the expression for S makes it possible to estimate the modal range for the occurrence of GOE statistics.

2. Natural frequencies of random plate structures

2.1. Plate with added masses and/or linear springs to ground

In this section, the equations of motion in modal space of a rectangular plate loaded by randomly located lumped masses and springs-to-ground are derived using the Lagrange–Rayleigh–Ritz technique [12]. The plate is simply supported, resulting in the following expression for the eigenfunctions $\phi_{mn}(\mathbf{x}) = \phi_m(x)\phi_n(y)$, where $\phi_m(x) = \sin(m\pi x/L_x)$ and $\phi_n(y) = \sin(n\pi x/L_y)$ are the shape functions in the x and y directions, respectively. m, n are, respectively, the mode numbers of the shape functions in the x and y directions. The flexural

displacement of the bare plate (in the absence of added mass) is given by

$$w(x,y,t)=\sum_{mn} q_{mn}(t)\psi_{mn}(\mathbf{x}) \tag{1}$$

where q_{mn} is the modal coordinate. $\psi_{mn}(\mathbf{x})=\psi_m(x)\psi_n(y)$ are the mass normalised mode shapes which satisfy the following orthogonality condition:

$$\int_0^{L_x}\int_0^{L_y}\rho h\psi_{mn}\psi_{m'n'}\,\mathrm{d}x\,\mathrm{d}y=\begin{cases}1, & mn=m'n'\\ 0, & mn\neq m'n'\end{cases} \tag{2}$$

L_x and L_y are, respectively, the lengths of the plate in the x and y directions, h is the plate thickness and ρ is the density. For a plate simply supported on all four sides, the mass-normalised eigenfunctions are given by

$$\psi_{mn}(\mathbf{x})=\frac{1}{\sqrt{M_n}}\phi_{mn}(\mathbf{x})=\frac{1}{\sqrt{M_n}}\sin\left(\frac{m\pi x}{L_x}\right)\sin\left(\frac{n\pi y}{L_y}\right) \tag{3}$$

where $M_n=\rho hL_xL_y/4$ is the modal mass. The kinetic energy of a plate with a single point mass located at $\mathbf{x}_a=(x_a,y_a)$ is given by

$$T=\frac{\rho h}{2}\int_0^{L_x}\int_0^{L_y}\dot{w}^2(\mathbf{x})\,\mathrm{d}x\,\mathrm{d}y+\frac{m_a}{2}\dot{w}^2(\mathbf{x}_a) \tag{4}$$

where the first term on the right hand side of Eq. (4) corresponds to the kinetic energy associated with the distributed mass of the plate and the second term corresponds to the kinetic energy associated with the discrete mass m_a. Using the orthogonality condition, an expression for the kinetic energy of the plate can be obtained as

$$T=\frac{1}{2}\sum_{mn}\dot{q}_{mn}^2+\frac{m_a}{2}\sum_{mn}\sum_{jk}\dot{q}_{mn}\dot{q}_{jk}\psi_{mn}(\mathbf{x}_a)\psi_{jk}(\mathbf{x}_a). \tag{5}$$

Similarly, for the simply supported plate loaded by a linear spring to ground of stiffness k_b and located at $\mathbf{x}_b=(x_b,y_b)$, an expression for the potential energy of the plate can be obtained as

$$V=\frac{1}{2}\sum_{mn}\omega_{mn}^2q_{mn}^2+\frac{k_b}{2}\sum_{mn}\sum_{jk}q_{mn}q_{jk}\psi_{mn}(\mathbf{x}_b)\psi_{jk}(\mathbf{x}_b) \tag{6}$$

where $\omega_{mn}=\sqrt{D/\rho h}((m\pi/L_x)^2+(n\pi/L_y)^2)$ corresponds to the natural frequencies of the bare plate and D is the flexural rigidity. Using Lagrange's equation for a particular modal coordinate pq of the bare plate in free vibration

$$\frac{\partial}{\partial t}\left(\frac{\partial T}{\partial\dot{q}_{pq}}\right)-\frac{\partial T}{\partial q_{pq}}+\frac{\partial V}{\partial q_{pq}}=0 \tag{7}$$

results in the following equation of motion for a mass and spring loaded plate:

$$\ddot{q}_{pq}+\sum_{mn}m_a\ddot{q}_{mn}\psi_{mn}(\mathbf{x}_a)\psi_{pq}(\mathbf{x}_a)+\sum_{mn}k_bq_{mn}\psi_{mn}(\mathbf{x}_b)\psi_{pq}(\mathbf{x}_b)+\omega_{pq}^2q_{pq}=0. \tag{8}$$

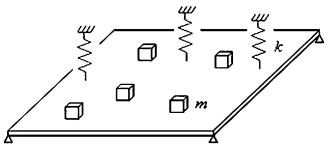

Fig. 1. A simply supported plate with randomly located point masses and springs to ground.

For the simply supported plate loaded by N_m number of point masses, and N_k linear springs as shown in Fig. 1, the equation of motion becomes

$$\ddot{q}_{pq} + \sum_{a=1}^{N_m} \sum_{mn} m_a \ddot{q}_{mn} \psi_{mn}(\mathbf{x}_a) \psi_{pq}(\mathbf{x}_a) + \sum_{b=1}^{N_k} \sum_{mn} k_b q_{mn} \psi_{mn}(\mathbf{x}_b) \psi_{pq}(\mathbf{x}_b) + \omega_{pq}^2 q_{pq} = 0. \tag{9}$$

For the mass and/or spring loaded plates, the natural frequencies were solved by the following eigenvalue analysis $(\mathbf{K} - \omega^2 \mathbf{M})\Psi = 0$. This was performed in MatLab using the command eig, which returns a diagonal matrix of eigenvalues and a matrix of corresponding eigenfunctions. In the absence of the added mass/stiffness, the equation of motion reduces to that for a homogeneous simply supported plate, corresponding to $\ddot{q}_{pq} + \omega_{pq}^2 q_{pq} = 0$. The mass and stiffness matrices for the bare plate are diagonal. The addition of point masses and/or springs leads to extra terms appearing in the off diagonal elements of the mass and stiffness matrices, respectively, due to the coupling between the eigenfunctions.

2.2. Plates coupled by springs

Consider two simply supported plates coupled by a linear spring of stiffness k at a random location $\mathbf{x}_i$ on each plate ($i = 1,2$ is the plate number). The total kinetic energy of the system is

$$T = \frac{\rho_1 h_1}{2} \int_0^{L_{x1}} \int_0^{L_{y1}} \dot{w}_1^2(\mathbf{x})\, \mathrm{d}x\, \mathrm{d}y + \frac{\rho_2 h_2}{2} \int_0^{L_{x2}} \int_0^{L_{y2}} \dot{w}_2^2(\mathbf{x})\, \mathrm{d}x\, \mathrm{d}y = \frac{1}{2} \sum_{mn} \dot{q}_{1,mn}^2 + \frac{1}{2} \sum_{mn} \dot{q}_{2,mn}^2 \tag{10}$$

Making use of the eigenfunction orthogonality conditions, the potential energy of the coupled plate system is given by

$$V = \frac{1}{2} \sum_{mn} \omega_{1,mn}^2 q_{1,mn}^2 + \frac{1}{2} \sum_{mn} \omega_{2,mn}^2 q_{2,mn}^2 + \frac{k}{2} (w_1(\mathbf{x}_1) - w_2(\mathbf{x}_2))^2 \tag{11}$$

where $\omega_{1,mn}$ and $\omega_{2,mn}$ are the natural frequencies of each uncoupled plate. The last term on the right hand side of Eq. (11) describes the coupling dynamics due to the randomly located spring. Differentiating the kinetic and potential energies with respect to the modal coordinate pq of the uncoupled plates and substituting into Lagrange's equation, the equations of motion for the spring-coupled plates are given by

$$\ddot{q}_{1,pq} + k\phi_{1,pq}(\mathbf{x}_1) \sum_{mn} q_{1,mn} \phi_{1,mn}(\mathbf{x}_1) - k\phi_{1,pq}(\mathbf{x}_1) \sum_{jk} q_{2,jk} \phi_{2,jk}(\mathbf{x}_2) + \omega_{1,pq}^2 q_{1,pq} = 0 \tag{12}$$

$$\ddot{q}_{2,pq} + k\phi_{2,pq}(\mathbf{x}_2) \sum_{jk} q_{2,jk} \phi_{2,jk}(\mathbf{x}_2) - k\phi_{2,pq}(\mathbf{x}_2) \sum_{mn} q_{1,mn} \phi_{1,mn}(\mathbf{x}_1) + \omega_{2,pq}^2 q_{2,pq} = 0 \tag{13}$$

Eqs. (12) and (13) can easily be expanded to account for N number of randomly located springs, as shown in Fig. 2. The natural frequencies of the spring-coupled plates were obtained by eigenvalue analysis using MatLab.

2.3. Plate with torsional edge springs

The equation of motion in modal space of a simply supported rectangular plate with torsional springs attached along the edges of the plate has been previously presented for a single spring located at each plate

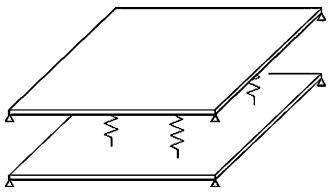

Fig. 2. Simply supported plates coupled by randomly located springs.

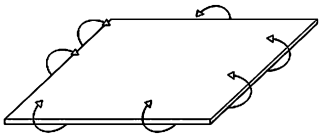

Fig. 3. Simply supported plate with randomly located torsional springs at its boundary edges.

edge [13]. For N_r number of torsional springs of stiffness K_t located at each simply supported edge corresponding to $(x_a,0)$, $(0,y_a)$, (x_b,L_y) and (L_x,y_b), as shown in Fig. 3, the equation of motion for a particular modal coordinate pq of the bare plate can be obtained as

$$\begin{aligned}\ddot{q}_{pq}&+\sum_{a=1}^{N_r}\sum_{mn}\frac{K_t}{M_n}q_{mn}\left(\frac{m\pi}{L_x}\right)\left(\frac{p\pi}{L_x}\right)\phi_n(y_a)\phi_q(y_a)+\sum_{a=1}^{N_r}\sum_{mn}\frac{K_t}{M_n}q_{mn}\left(\frac{n\pi}{L_y}\right)\left(\frac{q\pi}{L_y}\right)\phi_m(x_a)\phi_p(x_a)\\&+\sum_{b=1}^{N_r}\sum_{mn}\frac{K_t}{M_n}q_{mn}\left(\frac{m\pi}{L_x}\right)\left(\frac{p\pi}{L_x}\right)(-1)^m(-1)^p\phi_n(y_b)\phi_q(y_b)\\&+\sum_{b=1}^{N_r}\sum_{mn}\frac{K_t}{M_n}q_{mn}\left(\frac{n\pi}{L_y}\right)\left(\frac{q\pi}{L_y}\right)(-1)^n(-1)^q\phi_m(x_b)\phi_p(x_b)+\omega_{pq}^2q_{pq}=0\end{aligned}\tag{14}$$

where $M_n=\rho hL_xL_y/4$ is the modal mass. The natural frequencies of the plate with torsional edge springs were obtained by eigenvalue analysis using MatLab.

3. Statistical overlap factor applied to dynamic systems

3.1. Statistical overlap factor

The statistical overlap factor is defined by [11,14]

$$S=\frac{2\sigma}{\mu}=\frac{2\{\mathrm{var}[\Delta\omega_n]\}^{1/2}}{\mu}\tag{15}$$

where σ is the standard deviation of any particular natural frequency ω_n from its mean value due to uncertainties in the system, and is measured across an ensemble of random structures. μ is the mean frequency spacing (inverse of the modal density). Statistical overlap occurs when the random variation in an individual natural frequency of a system exceeds the mean frequency spacing. Manohar and Keane [11] showed that S can be related to the frequency beyond which the mean response of a structure exhibits stationary (non-oscillatory) behaviour. For coupled transversely vibrating beams or axially vibrating rods, oscillations in the statistics of the power spectra were shown to be caused by the occurrence of resonances as well as the variation of mode shape values at the coupling points and driving location for point forcing. The statistical overlap factor was used to identify the frequency beyond which the effect of individual natural frequencies and mode shapes ceased to dominate variations in the mean response. It was shown that for coupled beams, steady mean behaviour occurs for frequencies beyond a statistical overlap factor value of 2 for rain-on-the-roof excitation, and for frequencies beyond a statistical overlap factor value of 3 for point force excitation. For uncoupled systems, where the variation in the mean response is not affected by the mode shapes at the coupling point, a value of S greater than 1 for rain-on-the-roof excitation was shown to guarantee smooth mean behaviour. The statistical overlap factor is thereby a useful parameter to obtain a measure of the amount of mixing and veering that occurs between modes across an ensemble of nominally identical systems with uncertainties. In the following sections, approximate expressions for S for the mass and spring loaded plates are obtained by deriving the ensemble variance in the change of any particular natural frequency.

3.2. Perturbation analysis for a plate with added masses or linear springs

Using a first-order perturbation analysis, an approximate formula is developed for the ensemble variance in the change of any particular natural frequency, var[$\Delta\omega_{mn}$], which arises from adding point masses to the bare plate. The addition of N_m randomly located masses of size m_a to a plate will modify the mnth natural frequency of the bare plate as follows:

$$\omega_{mn}^2 \to \omega_{mn}^2\left[1 - \sum_{a=1}^{N_m} m_a \psi_{mn}^2(\mathbf{x}_a)\right] \tag{16}$$

and hence

$$\Delta\omega_{mn} \approx -\frac{\omega_{mn}}{2}\sum_a m_a \psi_{mn}^2(\mathbf{x}_a) \tag{17}$$

where $\psi_{mn}(\mathbf{x}) = \phi_{mn}(\mathbf{x})/\sqrt{M_n}$ and $\phi_{mn}(\mathbf{x}) = \phi_m(x)\phi_n(y)$. Eq. (18) follows from Rayleigh's quotient [12] on the assumption that the change in the natural frequency is small. Now if y_{mn} is defined as

$$y_{mn} = \sum_a m_a \psi_{mn}^2(\mathbf{x}_a) \tag{18}$$

and noting that $\mathrm{E}[\psi_{mn}^2] = 1/M$, where $M = 4M_n$ is the total mass of the bare plate, then the mean of y_{mn} becomes

$$\mathrm{E}[y_{mn}] = \sum_a m_a \mathrm{E}[\psi_{mn}^2(\mathbf{x}_a)] = \frac{N_m m_a}{M} \tag{19}$$

The variance of y_{mn} is given by

$$\mathrm{var}[y_{mn}] = \mathrm{E}[(y_{mn})^2] - \mathrm{E}[y_{mn}]^2 = \sum_a m_a^2(\mathrm{E}[\psi_{mn}^4(\mathbf{x}_a)] - \mathrm{E}[\psi_{mn}^2(\mathbf{x}_a)]^2) \tag{20}$$

Since the modes of the bare plate have been taken to be sinusoidal, so that $\mathrm{E}[\psi_{mn}^4] = (9/4)\mathrm{E}[\psi_{mn}^2]^2$ [15], the variance of y_{mn} becomes

$$\mathrm{var}[y_{mn}] = 1.25\frac{N_m m_a^2}{M^2} \tag{21}$$

From Eqs. (17)–(21), it now follows that the variance in the value of any particular natural frequency with the addition of N_m masses is given by

$$\sigma^2 = \mathrm{var}[\Delta\omega_{mn}] = \mathrm{var}[y_{mn}/2\omega_{mn}] = 0.3125\omega_{mn}^2\frac{N_m m_a^2}{M^2} \tag{22}$$

Thus, from Eq. (15), an approximate expression for the statistical overlap factor is obtained as

$$S = \frac{2\sigma}{\mu} \approx \frac{1.118\omega}{\mu}\left(\frac{1}{\sqrt{N_m}}\right)\left(\frac{N_m m_a}{M}\right) \tag{23}$$

For given m_a, N_m and M, the frequency ω as S approaches unity can be calculated, defining the modal range beyond which the occurrence of GOE statistics is expected to apply. The approximate expression for the statistical overlap factor given by Eq. (23) is based on a first-order perturbation analysis and serves as a useful guideline to the degree of statistical overlap at a specified frequency ω, or conversely, to the frequency at which the statistical overlap will first approach unity for the uncoupled system.

Similarly, an approximate formula for the statistical overlap factor arising from adding N_k linear springs to ground at random locations $\mathbf{x}_b$ on a simply supported plate can be developed. The mnth natural frequency of a bare plate is modified by the addition of N_k springs, each of stiffness k_b, as follows:

$$\omega_{mn}^2 \to \omega_{mn}^2 + \sum_{b=1}^{N_k} k_b \psi_{mn}^2(\mathbf{x}_b) \tag{24}$$

and hence

$$\Delta\omega_{mn} \approx \frac{1}{2\omega_{mn}} \sum_b k_b \psi_{mn}^2(\mathbf{x}_b) \tag{25}$$

where ψ_{mn} is the mnth mode shape of the bare plate scaled to unit generalised mass. Following a similar procedure for the mass loaded plate, an approximate expression for the statistical overlap factor for a linear spring loaded plate can be obtained as

$$S \approx \frac{1.118}{\mu\omega}\left(\frac{1}{\sqrt{N_k}}\right)\left(\frac{N_k k_b}{M}\right) \tag{26}$$

3.3. Perturbation analysis for a torsional edge spring loaded plate

In this section, an approximate formula for the statistical overlap factor is developed for the case of a simply supported plate loaded by N_r number of torsional springs at each edge (Fig. 3). For torsional edge springs, each of stiffness K_t, the mnth natural frequency of the bare plate is modified by

$$\omega_{mn}^2 \to \omega_{mn}^2 + \sum_{a=1}^{N_r} \frac{K_t}{M_n}\left(\left(\frac{m\pi}{L_x}\right)^2 \phi_n^2(y_a) + \left(\frac{n\pi}{L_y}\right)^2 \phi_m^2(x_a)\right) + \sum_{b=1}^{N_r} \frac{K_t}{M_n}\left(\left(\frac{m\pi}{L_x}\right)^2 \phi_n^2(y_b) + \left(\frac{n\pi}{L_y}\right)^2 \phi_m^2(x_b)\right) \tag{27}$$

and hence

$$\Delta\omega_{mn} \approx \frac{K_t}{2\omega_{mn} M_n} \sum_a \left(\left(\frac{m\pi}{L_x}\right)^2 \phi_n^2(y_a) + \left(\frac{n\pi}{L_y}\right)^2 \phi_m^2(x_a)\right) + \sum_b \left(\left(\frac{m\pi}{L_x}\right)^2 \phi_n^2(y_b) + \left(\frac{n\pi}{L_y}\right)^2 \phi_m^2(x_b)\right) \tag{28}$$

In this case let y_{mn} be defined as

$$y_{mn} = \frac{K_t}{M_n} \sum_a \left(\left(\frac{m\pi}{L_x}\right)^2 \phi_n^2(y_a) + \left(\frac{n\pi}{L_y}\right)^2 \phi_m^2(x_a)\right) + \sum_b \left(\left(\frac{m\pi}{L_x}\right)^2 \phi_n^2(y_b) + \left(\frac{n\pi}{L_y}\right)^2 \phi_m^2(x_b)\right) \tag{29}$$

Noting that $M = 4M_n$, the mean of y_{mn} becomes

$$\mathrm{E}[y_{mn}] = \frac{4N_r K_t}{M}\left\{\left(\frac{m\pi}{L_x}\right)^2 + \left(\frac{n\pi}{L_y}\right)^2\right\} \tag{30}$$

Also noting that $\mathrm{E}[\phi_n^4] = (3/2)\mathrm{E}[\phi_n^2]^2$ [15], it can be shown that

$$\mathrm{var}[y_{mn}] = \mathrm{E}[(y_{mn})^2] - \mathrm{E}[y_{mn}]^2 = \frac{4N_r K_t^2}{M^2}\left\{\left(\frac{m\pi}{L_x}\right)^4 + \left(\frac{n\pi}{L_y}\right)^4\right\} \tag{31}$$

$$\sigma = \{\mathrm{var}[\Delta\omega_{mn}]\}^{1/2} = \{\mathrm{var}[y_{mn}/2\omega_{mn}]\}^{1/2} = \frac{\sqrt{N_r} K_t}{\omega_{mn} M}\left\{\left(\frac{m\pi}{L_x}\right)^4 + \left(\frac{n\pi}{L_y}\right)^4\right\}^{1/2} \tag{32}$$

Eq. (32) can be further simplified in what follows: the x and y wavenumber components of the simply supported plate can be written in terms of the free plate wavenumber k_p and angle defining the direction of propagation of the free wave θ:

$$\left(\frac{m\pi}{L_x}\right) = k_p \cos\theta \tag{33}$$

$$\left(\frac{n\pi}{L_y}\right) = k_p \sin\theta \tag{34}$$

Averaging over θ results in

$$\left\{\left(\frac{m\pi}{L_x}\right)^4+\left(\frac{n\pi}{L_y}\right)^4\right\}^{1/2}=\frac{\sqrt{3}}{2}k_p^2 \tag{35}$$

The plate wavenumber can be expressed in terms of the mean frequency spacing (inverse of the modal density) by [15]

$$k_p^2=\frac{4\pi\omega}{\mu A} \tag{36}$$

where $A=L_xL_y$ is the area of the plate. Substituting Eqs. (36) and (35) into (32) shows that the standard deviation in the value of any particular natural frequency from its mean value across the ensemble is independent of frequency:

$$\sigma=\frac{2\sqrt{3}\pi\sqrt{N_r}K_t}{\mu AM} \tag{37}$$

Hence, the resulting approximate expression of the statistical overlap factor for the torsional edge spring loaded plate is also independent of frequency:

$$S=\frac{4\sqrt{3}\pi\sqrt{N_r}K_t}{\mu^2AM}\approx\frac{21.766}{\mu^2A}\left(\frac{1}{\sqrt{N_r}}\right)\left(\frac{N_rK_t}{M}\right) \tag{38}$$

4. Modal spacing statistics

The modal spacing statistics of a dynamic system with symmetries such as a perfect rectangular plate or a perfect box-shaped room results in the probability density function (*pdf*) of the spacings between successive natural frequencies described by an exponential distribution [4]:

$$p(s)=a\mathrm{e}^{-as},\quad s\geqslant 0 \tag{39}$$

where $a=1/\mu$ and μ is the mean spacing between neighbouring natural frequencies. A significant characteristic of an exponential distribution is the absence of repulsion between modes, that is, $p(0)\neq 0$. The mean spacing can be estimated analytically as the inverse of the modal density, which is known for many types of simple systems.

The natural frequencies of a random system are more accurately described by GOE statistics. One feature of the GOE is that the distribution of the spacing between successive natural frequencies is Rayleigh, also known as the "Wigner surmise" of random matrix theory [5]. The probability density of the Rayleigh function is given by

$$p(s)=\frac{s}{c^2}\,\mathrm{e}^{-s^2/2c^2},\quad s\geqslant 0 \tag{40}$$

where $c=\mu\sqrt{2/\pi}$. A characteristic of the Rayleigh distribution is the presence of repulsion, that is, $p(0)=0$, due to veering between closely spaced modes, which results in a reduced probability of small frequency spacings. Exponential and Rayleigh distributions are shown in Figs. 4(a) and (b), respectively.

The closeness of a modal spacing distribution to the exponential and Rayleigh distributions can be observed using a probability plot, in which the modal spacing distribution is plotted against a theoretical distribution to approximately form a straight line. The horizontal axis of the probability plot is the ordered statistic medians $N(i)$ for the given distribution which are determined by [16]

$$N(i)=G(U(i)) \tag{41}$$

G is the inverse of the cumulative distribution function and $U(i)$ are the uniform ordered statistic medians. The inverse of the cumulative distribution function for the Rayleigh and exponential distributions are respectively

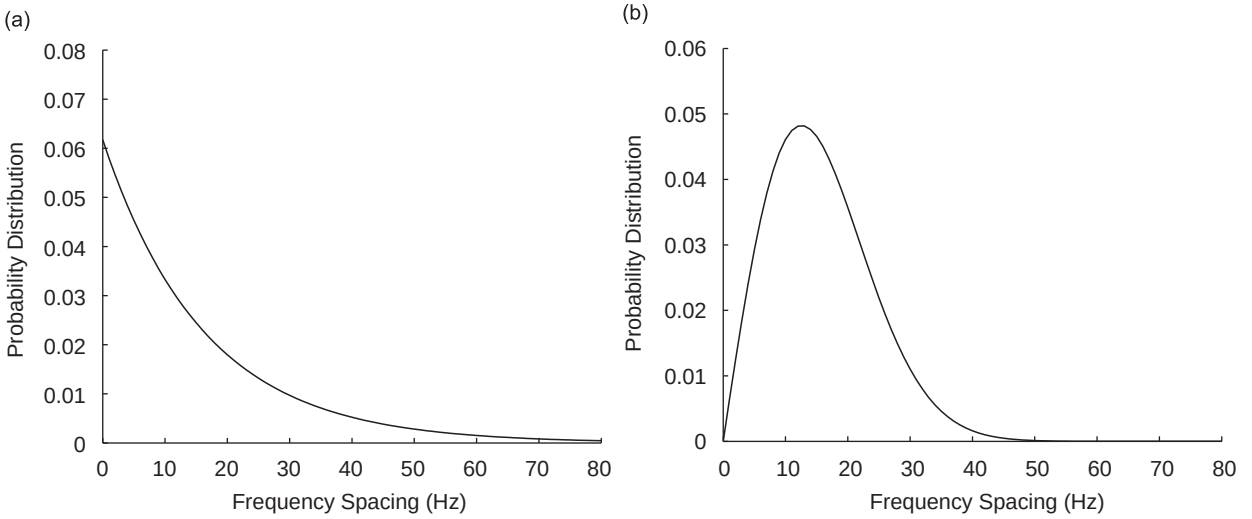

Fig. 4. (a) Exponential distribution. (b) Rayleigh distribution.

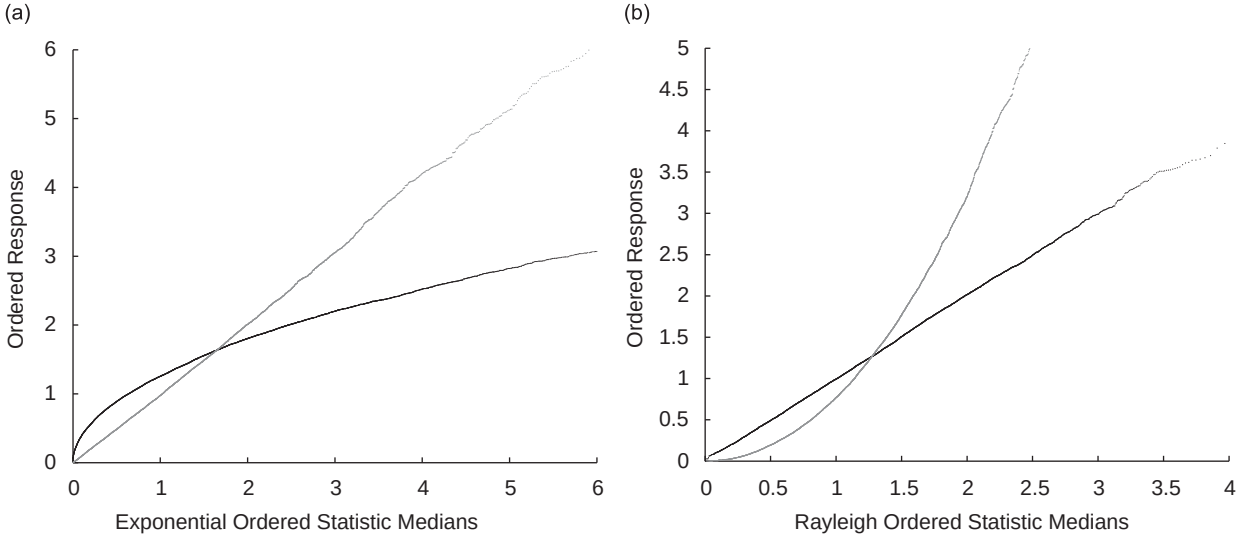

Fig. 5. (a) Exponential probability plot with a Rayleigh distribution (black line) and an exponential distribution (grey line). (b) Rayleigh probability plot with a Rayleigh distribution (black line) and an exponential distribution (grey line).

given by [17]

$$s = c\sqrt{-2\ln(1-U(i))} \tag{42}$$

$$s = \frac{-\ln(1-U(i))}{a} \tag{43}$$

The uniform ordered statistic medians are defined as [16]

$$U(1) = 1 - U(n) \tag{44}$$

$$U(i) = \frac{(i-0.3175)}{(n+0.365)} \quad \text{for } i = 2,3,\ldots,n-1 \tag{45}$$

$$U(n) = 0.5^{1/n} \tag{46}$$

The vertical axis of the probability plot is the modal spacings arranged in increasing order. Rayleigh and exponential distributions are shown in Fig. 5(a) on an exponential probability plot. This figure illustrates that a true exponential distribution will exhibit a straight line with a 1:1 slope, although some deviation from a straight line generally occurs at high values. In a Rayleigh probability plot shown in Fig. 5(b), the Rayleigh distribution shows a straight line with a 1:1 slope while the exponential distribution deviates.

5. Results

Simulation results are presented for several ensembles of structures corresponding to a mass-loaded plate, a linear spring-loaded plate, a mass-and-spring-loaded plate, two plates coupled by linear springs and a plate with torsional springs. For the first three structures involving added masses and/or linear springs to ground, rectangular simply supported plates of dimensions $L_x = 899\,\text{mm}$, $L_y = 600\,\text{mm}$ and thickness $h = 2\,\text{mm}$, with material properties of aluminium (density $\rho = 2800\,\text{kg/m}^3$, Young's modulus $E = 70\,\text{GPa}$, Poisson's ratio $v = 0.3$) were used. Damping was included in the analysis by using a complex Young's modulus $E(1+j\eta)$ where $\eta = 0.1$ percent is the structural loss factor. Various combinations were investigated for different numbers and values of the added masses and linear springs. Fifty ensembles were generated by adding the masses and/or linear springs at random locations to each plate. Initially, ensembles consisting of 5, 10, 20 and 50 added masses and/or springs to ground were examined; where the masses are 0.2 percent of the bare plate mass M and the linear springs have stiffness 0.5 MN/m. In addition, three more ensembles were examined such that the degree of randomness is constant for each ensemble. The degree of randomness is given by $R = N_m m_a$ or $R = N_k k_b$. The three ensembles for the various plate structures with constant degree of randomness are presented in Table 1. For the structure consisting of two plates coupled by linear springs, the same plate dimensions and material parameters for the mass and/or spring loaded plates were used, with coupling springs of stiffness 5 MN/m. Fifty ensembles were generated by randomising the location of the coupling springs on each plate. A rectangular steel plate with torsional springs at its boundary edges on all four sides was also examined. Plate dimensions of $L_x = 1350\,\text{mm}$, $L_y = 1200\,\text{mm}$ and thickness $h = 5\,\text{mm}$, with material properties of steel (density $\rho = 7800\,\text{kg/m}^3$, Young's modulus $E = 210\,\text{GPa}$, Poisson's ratio $v = 0.3$) were used. Damping was included in the analysis by using a complex Young's modulus $E(1+j\eta)$ where $\eta = 0.1$ percent is the structural loss factor. N_r number of torsional springs of stiffness K_t were added on each edge. Fifty ensembles were generated by locating the torsional springs at random positions along the edges of the plate. For each of the aforementioned ensembles, the mean natural frequencies, their standard deviation and the mean frequency spacing across the ensemble were calculated.

5.1. Mass-loaded plate

The statistical overlap factor curves for a mass-loaded plate are shown in Fig. 6. The ensembles consist of 5, 10, 20 and 50 added masses, where each mass is 0.2 percent of the bare plate mass. There is a steady increase in statistical overlap factor with both increasing frequency and increasing randomness (defined by a greater

Table 1
Ensembles for the various plates with mass and stiffness perturbations.

Ensemble	Structure		
	Mass-loaded plate	Spring-loaded plate	Mass-and-spring-loaded plate
1	$N_m = 1$, $m = 10\%$ of the bare plate mass	$N_k = 1$, $k = 25\,\text{MN/m}$	$N_m = 1$, $m = 10\%$ of the bare plate mass; $N_k = 1$, $k = 25\,\text{MN/m}$
2	$N_m = 10$, $m = 1\%$ of the bare plate mass	$N_k = 10$, $k = 2.5\,\text{MN/m}$	$N_m = 10$, $m = 1\%$ of the bare plate mass; $N_k = 10$, $k = 2.5\,\text{MN/m}$
3	$N_m = 50$, $m = 0.2\%$ of the bare plate mass	$N_k = 50$, $k = 0.5\,\text{MN/m}$	$N_m = 50$, $m = 0.2\%$ of the bare plate mass; $N_k = 50$, $k = 0.5\,\text{MN/m}$

Each ensemble has a constant degree of randomness.

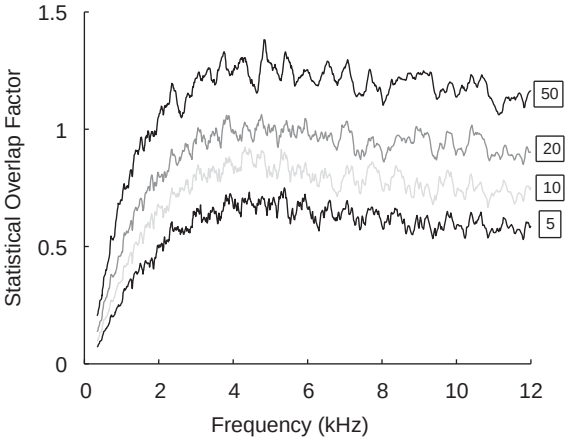

Fig. 6. Statistical overlap factor for a plate with 5, 10, 20 and 50 added masses of the same value.

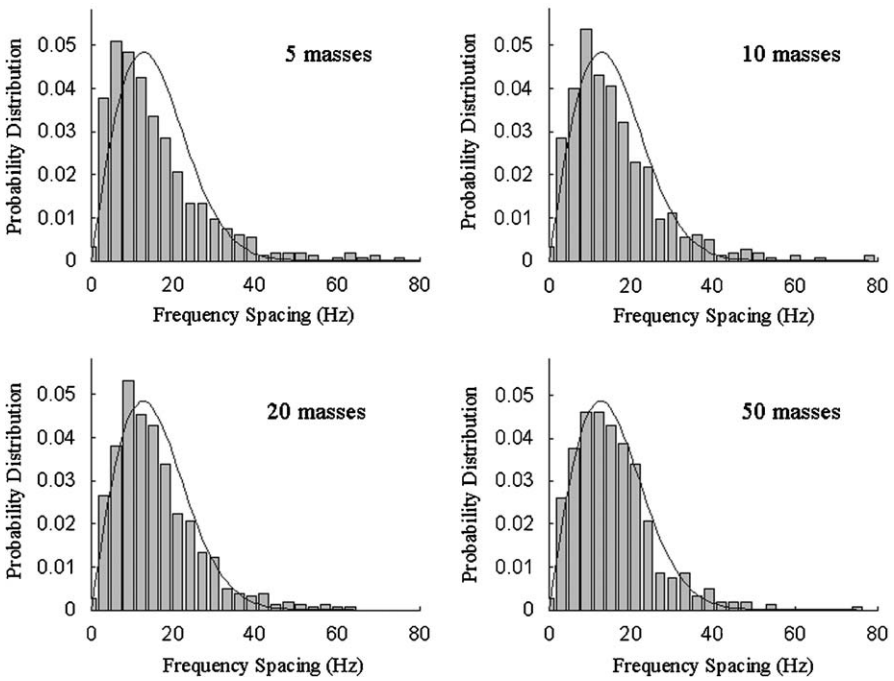

Fig. 7. Rayleigh distribution (black line) and *pdf* of the natural frequency spacings for a plate 5, 10, 20, and 50 added masses of the same value. Frequency range is 3–12 kHz.

number of added masses N_m for a given size m_a). The linear increase in the statistical overlap factor with frequency is confirmed by the first-order perturbation analysis for a mass-loaded plate given by Eq. (21). Furthermore, the slope of the curves becomes steeper as the number of added masses increases. Small values for the statistical overlap factor at lower frequencies is due to the fact that the lower modes are in well defined positions, that is, the natural frequencies move by only a relatively small amount from their mean value. As the frequency increases, the dynamic system becomes more sensitive to any structural uncertainty. The natural frequencies move significantly and veer from one another, resulting in larger values for S. For each ensemble, the curves for S tend to level off. This is attributed to the fact that as the frequency increases, the inertia force generated by each mass also increases, until the masses effectively act as point constraints. The action of a constraint by the added masses involves several mode shapes combining to produce a zero displacement at the

constraint. This indicates that the results for S have saturated such that no further increase in statistical overlap will occur with increasing frequency. Interestingly, whilst S levels off at a higher value for a greater number of added masses, the frequency at which the curves for all masses level off is approximately the same in each case. Fig. 6 shows that for a mass-loaded plate, increasing the number of masses results in a greater degree of variation in the position of the natural frequencies.

Fig. 7 presents the *pdf* of the natural frequency spacings for one member from each of the four ensembles of the mass-loaded plates. A *pdf* of the modal spacings for each dynamic system was obtained as follows: the natural frequencies obtained from eigenvalue analysis of the equation of motion were arranged in ascending order and the spacings between successive frequencies were obtained. The top 20 percent of modes were discarded as the modal spacing was found to greatly increase for the highest order modes [12]. A histogram of the natural frequency spacings was then generated and converted to a *pdf* by scaling to unit area. The mean frequency spacing for each ensemble member was also calculated. The *pdf* of the natural frequency spacings for a given modal range was then curve fitted with a Rayleigh spacing distribution using the mean frequency spacing from an ensemble member for each of the mass-loaded plates. Increasing the number of masses did not significantly affect the mean frequency spacing of the mass-loaded plates, which ranged from 15.7 Hz for 5 added masses to 15.6 Hz for 50 added masses. The probability distributions are presented for a frequency range from 3 to 12 kHz, which approximately corresponds to the region shown in Fig. 6 where S begins to level off for each ensemble. At lower frequencies, the modes are in well defined positions and hence will not significantly contribute to any structural uncertainty. Fig. 8 shows a Rayleigh probability plot of the ordered natural frequency spacings. The probability plot was generated by arranging the natural frequency spacings in order and plotting them in relation to ordered statistic medians generated from a Rayleigh distribution. Figs. 7 and 8 show that as the number of masses increases and hence S increases, the distribution of the modal spacings results in the closest match with a Rayleigh distribution.

The statistical overlap factors for the ensembles of a mass-loaded plate presented in Table 1, corresponding to the case where each ensemble has the same degree of randomness, are shown in Fig. 9. S initially increases with frequency for an increasing number of added masses, even though the amount of the added mass is

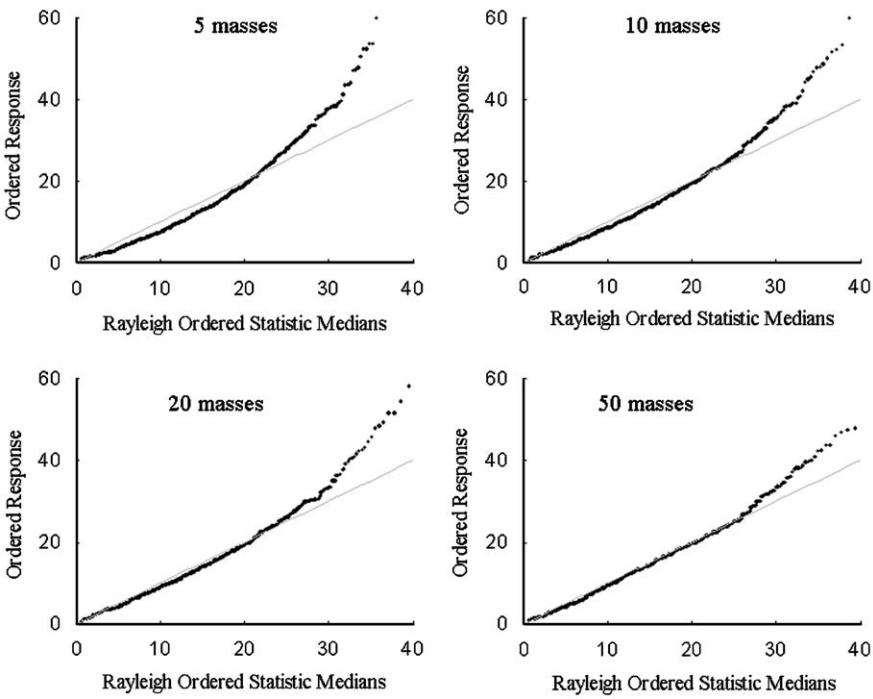

Fig. 8. Rayleigh probability plot of the ordered response (black points) and Rayleigh distribution line (grey line) of the frequency spacings for a plate with 5, 10, 20, and 50 added masses of the same value. Frequency range is 3–12 kHz.

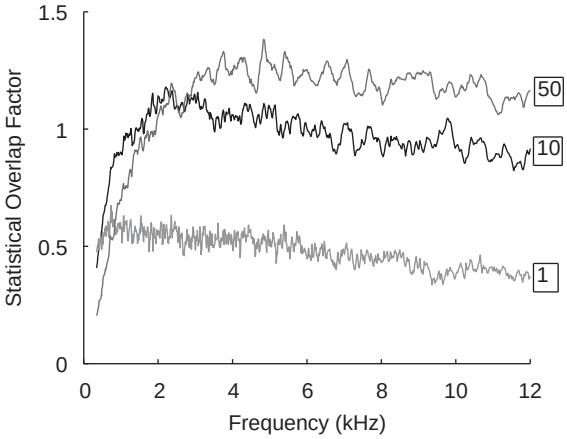

Fig. 9. Statistical overlap factor for a plate with 1, 10 and 50 added masses of different values, such that each ensemble has the same degree of randomness.

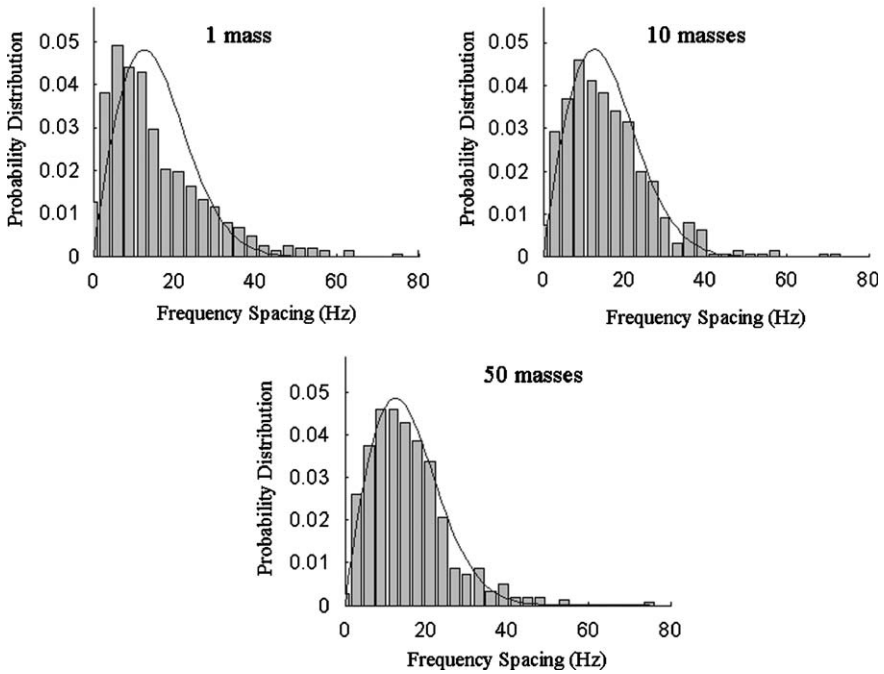

Fig. 10. Rayleigh distribution (black line) and *pdf* of the natural frequency spacings for a plate with 1, 10 and 50 added masses of different values. Frequency range is 3–12 kHz.

decreasing. In each case, the curves for S level off. For 10 and 50 added masses, S levels off at approximately the same frequency, indicating the frequency range beyond which the results have saturated such that the response becomes independent of the type of uncertainty. For a single added mass, S is relatively constant at all frequencies and significantly less than unity, indicating there is insufficient structural uncertainty for the modes to mix and veer from one another. Fig. 10 shows the *pdf* of the natural frequency spacings for each dynamic system in the frequency range from 3 to 12 kHz. These *pdf*s are compared to a Rayleigh distribution using the mean frequency spacing, corresponding to 15.8, 15.7 and 15.6 Hz for 1, 10 and 50 added masses, respectively. For the ensembles presented, the greater statistical overlap factor occurs for 50 added masses, resulting in the closest match to a Rayleigh distribution. These results are further confirmed in Fig. 11, which

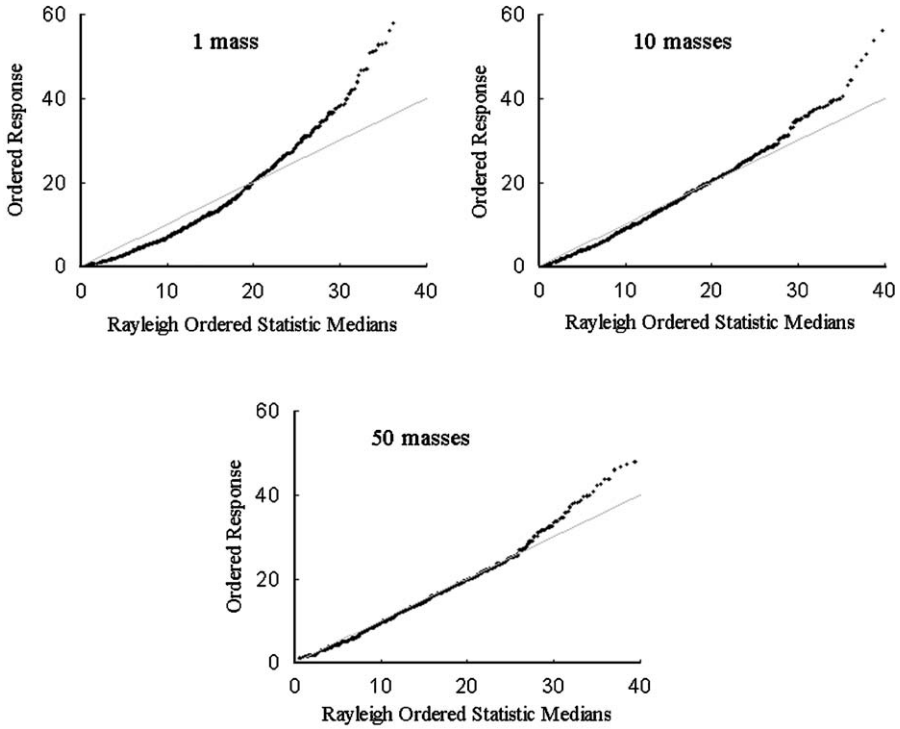

Fig. 11. Rayleigh probability plot of the ordered response (black points) and Rayleigh distribution line (grey line) of the frequency spacings for a plate with 1, 10 and 50 added masses of different values. Frequency range is 3–12 kHz.

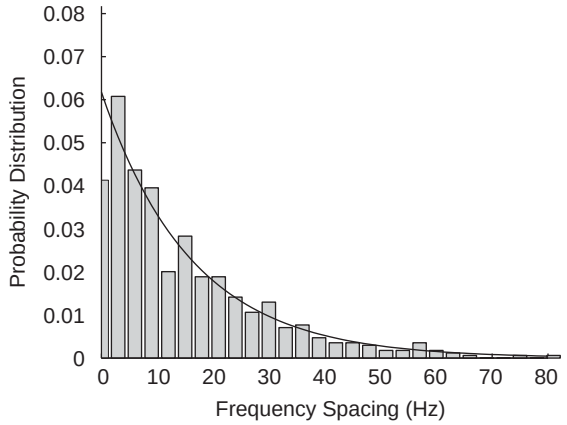

Fig. 12. Exponential distribution (black line) and *pdf* of the natural frequency spacings for a bare plate.

shows the ordered natural frequencies of a Rayleigh probability plot. The results for these ensembles demonstrate that the value of S will increase for a greater number of perturbations, even though the degree of randomness is the same in each case.

To compare the modal spacing statistics for dynamic systems with and without structural uncertainty, the modal statistics of a bare simply supported rectangular plate was obtained. The modal density of the bare plate (in the absence of added mass/stiffness) was calculated by $n=(L_xL_y/4\pi)\sqrt{\rho h/D}$, where $D=Eh^3/12(1-v^2)$ is the flexural rigidity. An aluminium plate of dimensions $L_x=899\,\text{mm}$, $L_y=600\,\text{mm}$ and thickness $h=2\,\text{mm}$ results in a mean frequency spacing of $\mu=1/n\approx 70.5\,\text{rad/s}$ (11.2 Hz). Using the Rayleigh–Ritz–Lagrange technique, the natural frequencies of the bare plate were obtained from eigenvalue

analysis of the equation of motion, arranged in ascending order, and the spacings between successive frequencies obtained. The mean frequency spacing of the bare plate was calculated to be approximately 11 Hz, which is in excellent agreement with the predicted modal spacing. The *pdf* of the natural frequency spacings was then curve fitted to an exponential distribution, given by Eq. (39). Fig. 12 clearly shows that a dynamic system with symmetries, as in the case of a bare simply supported rectangular plate, exhibits no repulsion between modes and is described by an exponential distribution.

5.2. Spring-loaded plate

The statistical overlap factor curves for a spring-loaded plate are shown in Fig. 13. The ensembles consist of 5, 10, 20 and 50 added linear springs to ground, each of stiffness 0.5 MN/m. Fifty configurations for each ensemble were generated by attaching the springs at random locations across the surface of the plate. In Fig. 13, the statistical overlap factor for each of the ensembles begins at a high value and then decreases rapidly as frequency increases. All curves tend towards zero at high frequencies. This is attributed to the fact that at higher frequencies, springs have less effect on the variation in the natural frequencies than at lower frequencies. The inverse proportionality of the statistical overlap factor with frequency for spring-loaded plates is confirmed by the approximate expression for S given by the perturbation analysis (Eq. (26)). Fig. 14 presents the *pdf* of the natural frequency spacings for one member of each of the ensembles in the frequency range from 200 Hz to 6 kHz. Fig. 14 also shows the Rayleigh distribution calculated using the mean frequency spacings for each ensemble corresponding to 11.8, 11.7, 11.7 and 11.5 Hz for 5, 10, 20 and 50 added springs, respectively. Fig. 15 presents the Rayleigh probability plot of the ordered natural frequency spacings in the frequency range 200 Hz to 6 kHz. Figs. 14 and 15 indicate that the spring-loaded plates do not generate sufficient randomness of the natural frequencies to result in a clear Rayleigh distribution of the modal spacings. The closest match of the *pdf* of the modal spacings to a Rayleigh distribution is for 50 added springs. The effect of added linear springs to ground is to vary the positions of the natural frequencies at low frequencies, although this effect is rapidly diminished with increasing frequency. However, the addition of linear springs to ground to the mass-loaded plates will have the effect of randomising the low order modes, thus extending the modal range for the occurrence of GOE statistics to lower frequencies. This is examined in the next section (Section 5.3).

The statistical overlap factors for the ensemble of a spring-loaded plate presented in Table 1, corresponding to the case where each ensemble has the same degree of randomness, are shown in Fig. 16. It can be seen that as the stiffness of the springs increases, the curves for S flatten. Similar to the case for a mass-loaded plate with only one added mass, the S curve for a spring-loaded plate with only one added linear spring to ground is relatively constant with frequency (and at a low value). The addition of just one spring (or mass) does not generate enough uncertainty to result in variation of the natural frequencies from their mean value across the

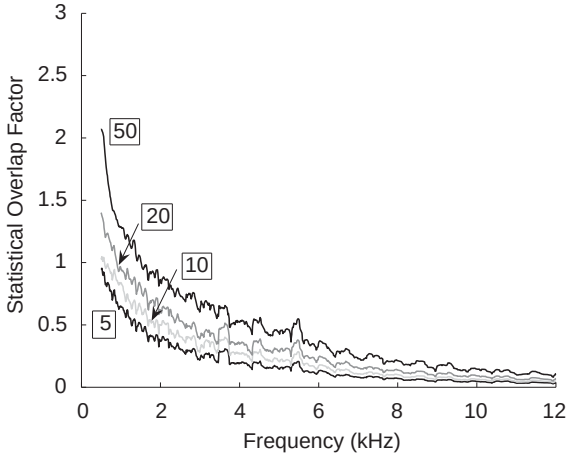

Fig. 13. Statistical overlap factors for a plate with 5, 10, 20 and 50 added linear springs to ground of the same stiffness.

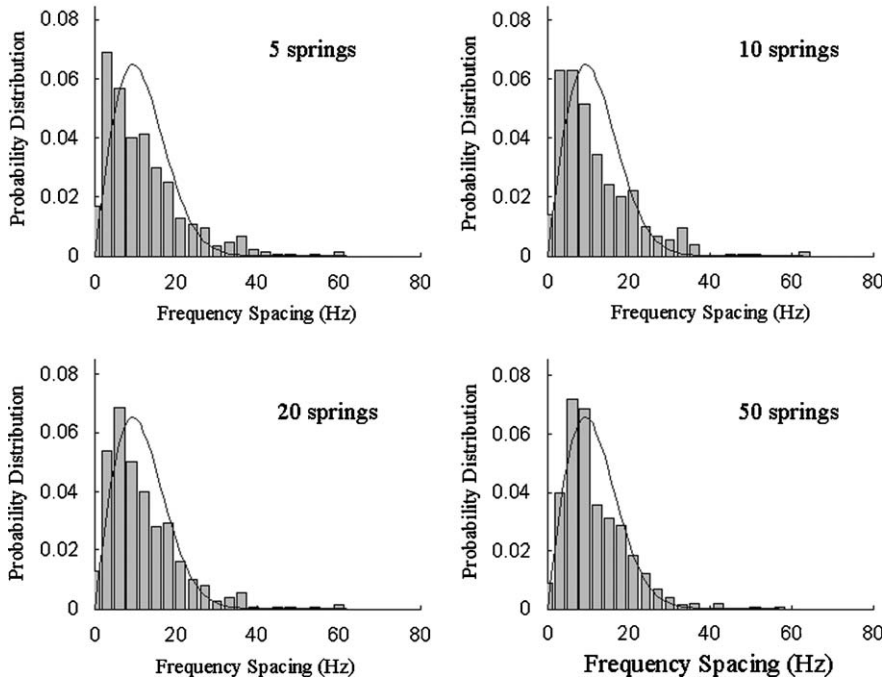

Fig. 14. Rayleigh distribution (black line) and *pdf* of the natural frequency spacings for a plate with 5, 10, 20, and 50 added linear springs to ground of the same stiffness. Frequency range is 200 Hz to 6 kHz.

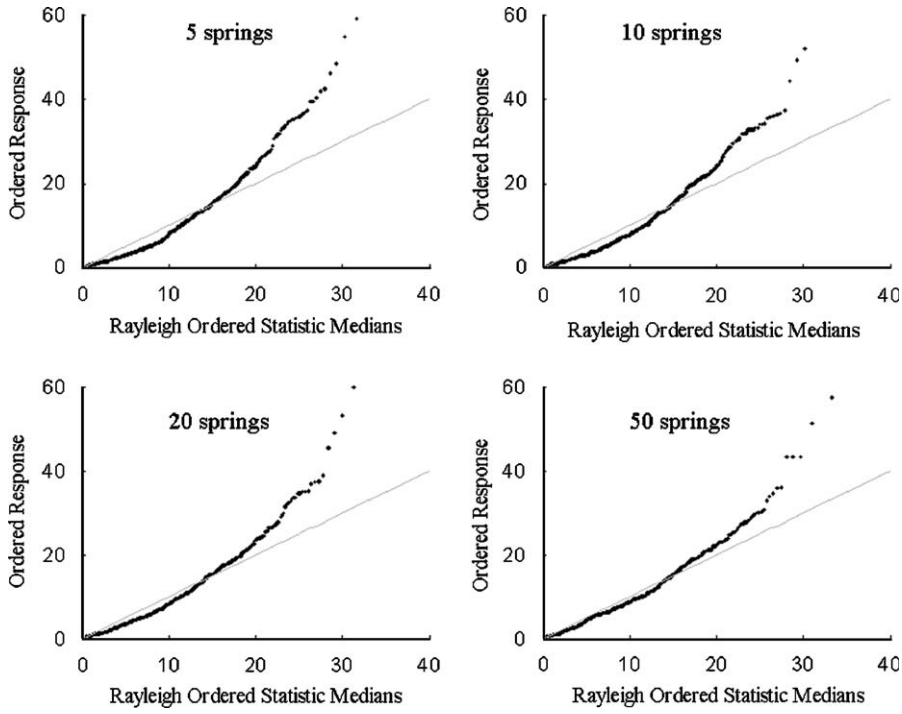

Fig. 15. Rayleigh probability plot of the ordered response (black points) and Rayleigh distribution line (grey line) of the frequency spacings for a plate with 5, 10, 20, and 50 linear springs to ground of the same stiffness. Frequency range is 200 Hz to 6 kHz.

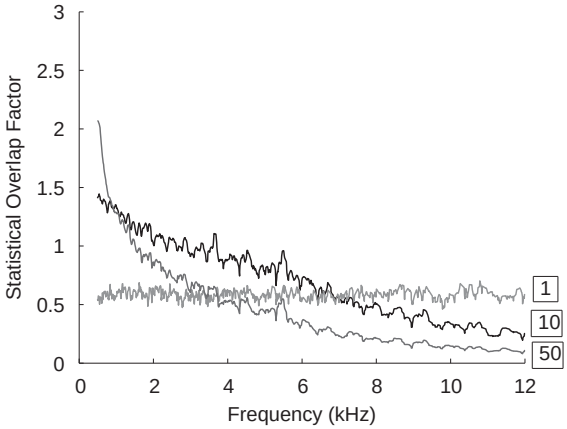

Fig. 16. Statistical overlap factor for a plate with 1, 10 and 50 added linear springs to ground of different stiffness such that each ensemble has the same degree of randomness.

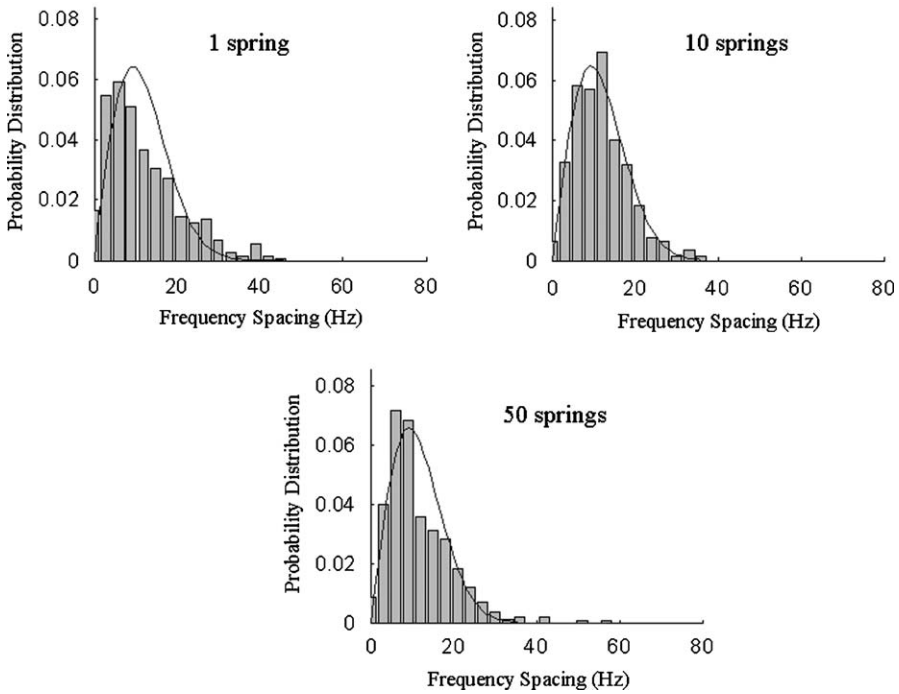

Fig. 17. Rayleigh distribution (black line) and *pdf* of the natural frequency spacings for a plate with 1, 10 and 50 added linear springs to ground of different stiffness. Frequency range is 200 Hz to 6 kHz.

ensemble. Increasing the number of springs results in an initially high value of S, even though the stiffness of the springs is decreased. The stiffness of the springs also affects the slope of S, particularly at low frequencies. Fig. 17 compares the natural frequency spacing distributions for each ensemble to Rayleigh distributions calculated using the mean frequency spacing for each ensemble, for the frequency range from 200 Hz to 6 kHz. In this frequency range, the mean frequency spacings are 11.8, 11.7 and 11.5 Hz for 1, 10 and 50 added springs. The *pdf* of the modal spacings for the ensemble with the greatest statistical overlap in this frequency region, corresponding to a plate with 10 added linear springs to ground, provides the closest match to a Rayleigh distribution. These results are further confirmed in Fig. 18, which compares the ordered natural frequencies of the Rayleigh probability plot to a Rayleigh distribution line. It is interesting to note that for a spring-loaded

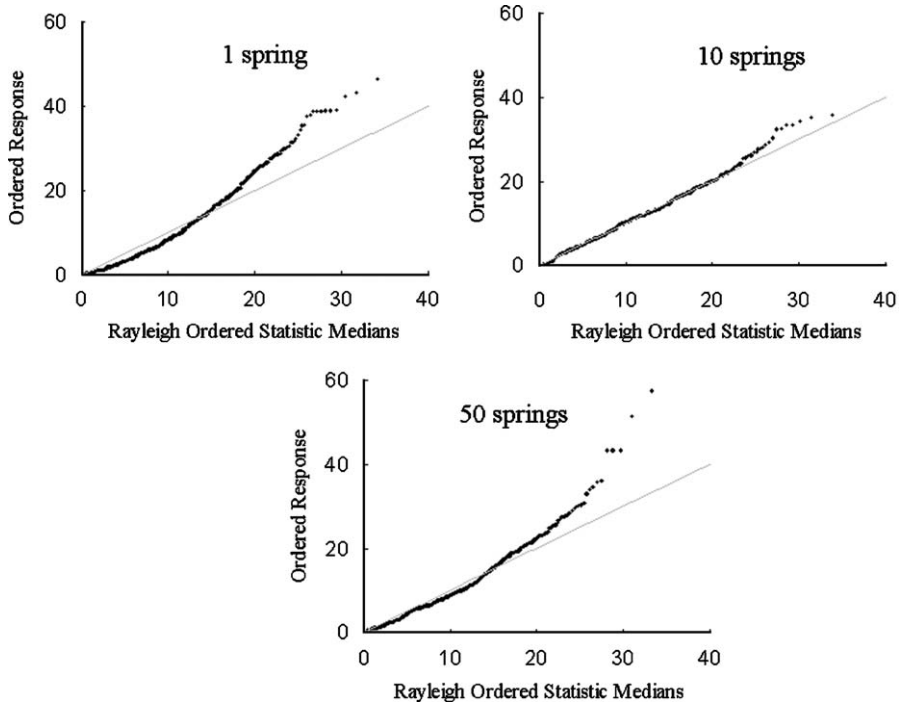

Fig. 18. Rayleigh probability plot of the ordered response (black points) and Rayleigh distribution line (grey line) of the frequency spacings for a plate with 1, 10 and 50 linear springs to ground of different stiffness. Frequency range is 200 Hz to 6 kHz.

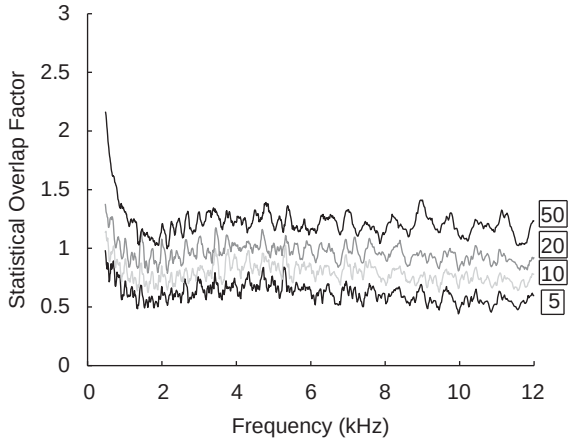

Fig. 19. Statistical overlap factor for a plate with 5, 10, 20 and 50 added masses of the same value and linear springs to ground of the same stiffness.

plate, a greater number of added springs do not generate a better Rayleigh distribution and this is attributed to the very low stiffness of the attached springs. As the springs decrease in stiffness, their effect on the low frequency plate modes also decreases.

5.3. Mass-and-spring-loaded plate

The statistical overlap factor curves for a mass-and-spring-loaded plate are shown in Fig. 19. The ensembles correspond to plates with 5, 10, 20 and 50 added masses and linear springs to ground, and were generated by randomising the positions of the masses and springs. Each mass is 0.2 percent of the bare plate mass and each

spring has a stiffness of 0.5 MN/m. In Fig. 19, for each of the ensembles, S begins at a high value, decreases and then levels off to a constant value. The larger the amount of added uncertainty, the greater the initial value of S at a low frequency. This is attributed to the added springs, which affect the variation of the low order modes. For the frequency beyond which a dip in the S curves occurs, the added masses are responsible for the variation in the natural frequencies. This is due to the inertia of the masses becoming more significant as frequency increases. When the statistical overlap factor curves level off, this indicates the frequency beyond which the results have saturated, such that the natural frequency statistics have become independent of the frequency and type of uncertainty. The addition of both masses and springs to a plate has resulted in the S curves becoming flatter with frequency when compared to the results for the mass-loaded plates (Fig. 6) and spring-loaded plates (Fig. 13).

Fig. 20 presents the *pdf* of the natural frequency spacings for one member from each of the four ensembles. Also shown in Fig. 20 are the Rayleigh distributions which were calculated using mean frequency spacings of 14.5, 14.5, 14.4 and 14.2 Hz for 5, 10, 20 and 50 added masses and springs, respectively. The mean frequency spacings, *pdf*s and Rayleigh distributions were obtained for a frequency range from 300 Hz to 12 kHz, that is, for the entire frequency range. A Rayleigh probability plot of the ordered natural frequency spacings is compared to a Rayleigh distribution line in Fig. 21. In Figs. 20 and 21, a closer match to a Rayleigh distribution is observed as the number of masses and springs increases.

The statistical overlap factors for the ensembles of a mass-and-spring-loaded plate presented in Table 1, corresponding to the case where each ensemble has the same degree of randomness, are shown in Fig. 22. Similar to the results presented previously for a mass or spring loaded plate, the statistical overlap for a plate with only a single added mass and linear spring to ground is relatively constant with frequency and at a low value. For a plate with a greater number of added masses and springs, S has a higher initial value which is attributed to the effect of the springs. As the frequency increases, a higher S value also occurs for a greater number of added masses. The slope of S is also affected by the different values and stiffness of the added masses and springs. Fig. 23 compares the *pdf* of the natural frequency spacings for each dynamic system to a

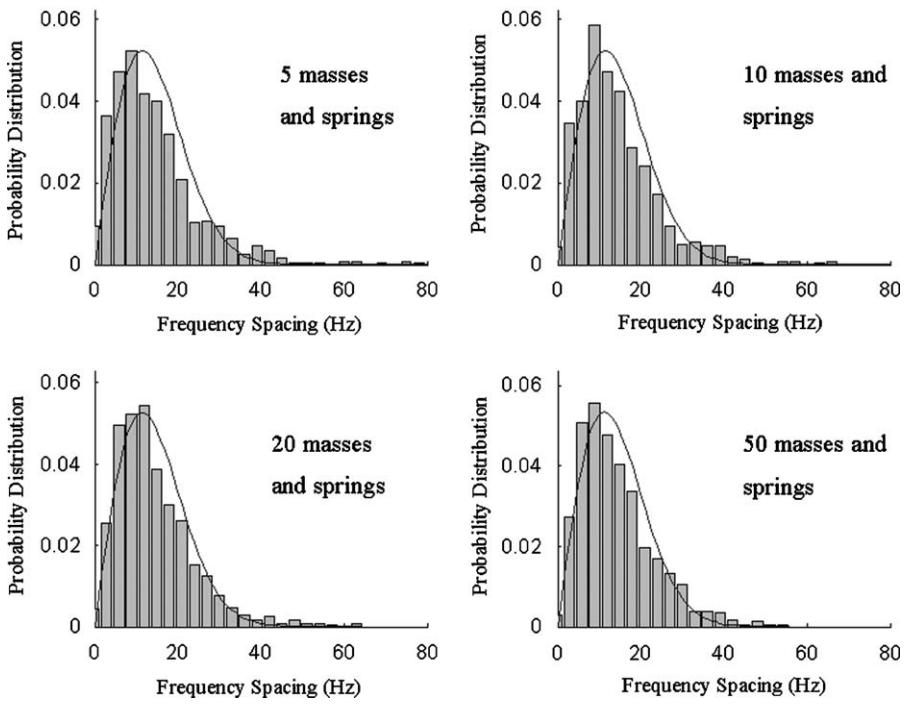

Fig. 20. Rayleigh distribution (black line) and *pdf* of the natural frequency spacings for a plate with 5, 10, 20, and 50 masses and linear springs to ground of the same size and stiffness. Frequency range is 300 Hz to 12 kHz.

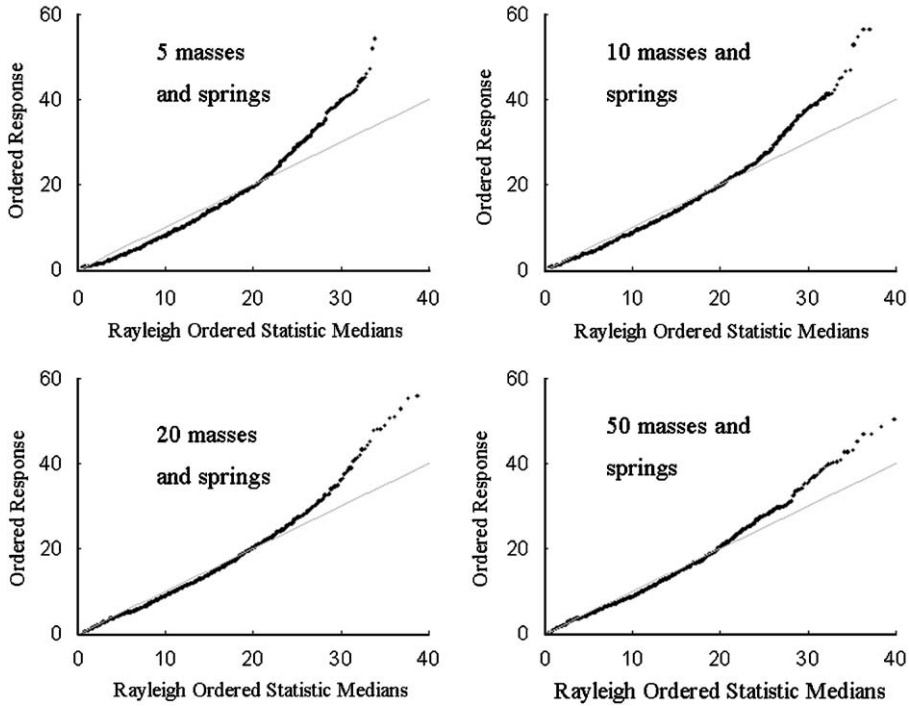

Fig. 21. Rayleigh probability plot of the ordered response (black points) and Rayleigh distribution line (grey line) of the frequency spacings for a plate with 5, 10, 20, and 50 added masses and linear springs to ground of the same value and stiffness. Frequency range is 300 Hz to 12 kHz.

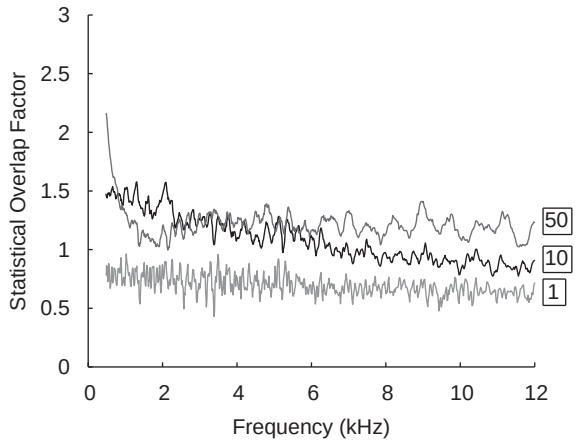

Fig. 22. Statistical overlap factor for a plate with 1, 10 and 50 added masses and linear springs to ground of different values and stiffness, such that each ensemble has the same degree of randomness.

Rayleigh distribution calculated using mean frequency spacings of 14.6, 14.5 and 14.2 Hz for 1, 10 and 50 added masses and springs. The mean frequency spacings, *pdf*s and Rayleigh distributions were obtained for a frequency range from 300 Hz to 12 kHz. The *pdf*s of the modal spacings for both 10 and 50 added masses and springs are very similar and are further confirmed by Fig. 24, which presents the closeness of the Rayleigh probability distributions to a Rayleigh distribution line. The similarity between the results in adding 10 and 50 masses and springs to a plate such that the degree of randomness is the same is attributed to the fact that

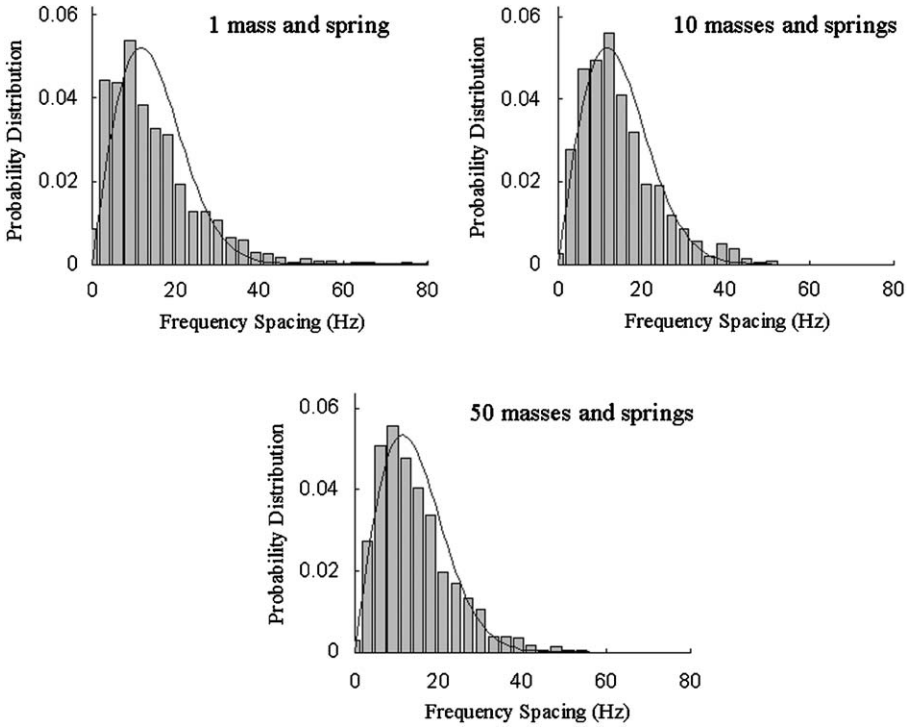

Fig. 23. Rayleigh distribution (black line) and *pdf* of the natural frequency spacings for a plate with 1, 10 and 50 masses and linear springs to ground of different values and stiffness. Frequency range is 300 Hz to 12 kHz.

both masses and springs are used to vary the properties of the plate, which affects both the low and high frequency modes. The values of the added masses and stiffness of the springs also affect the natural frequency statistics.

An interesting result for the statistical overlap factor for a mass-and-spring-loaded plate with collocated masses and springs is presented in Fig. 25. Fifty masses and collocated linear springs to ground were added at random locations, where the amount of each mass is 0.2 percent of the bare plate mass and the springs each have stiffness of 0.5 MN/m. Fig. 25 shows that there is a distinct dip in the statistical overlap factor curve at which the value for S is nearly zero. The frequency at which this dip occurs corresponds to the natural frequency for an equivalent single dof spring-mass system in terms of the added masses and springs, that is, $\omega_n = \sqrt{k_b N_k / m_a N_m} \approx 9098\,\mathrm{rad/s}$ (1448 Hz). At this frequency, the impedance of the added masses and springs is low and hence are not generating significant structural uncertainty on the plate. If $m_a N_m \gg k_b N_k$ such that $\omega_n \approx 0$, then the S curves would tend towards those shown in Fig. 6 for added masses only. Conversely, if $m_a N_m \ll k_b N_k$ such that $\omega_n \to \infty$, the S curves would tend towards those shown in Fig. 13 for added springs only.

5.4. Two plates coupled by springs

The statistical overlap factor for two plates coupled by linear springs are shown in Fig. 26. The ensembles consist of two plates coupled by 5, 10, 20 and 50 springs, where each spring has a stiffness of 5 MN/m. The statistical overlap factor for each of the ensembles is mainly constant across the frequency range from 300 Hz to 5 kHz. This indicates that the value of S has become saturated and will not significantly increase as frequency increases. However, the value of S increases for a greater number of coupling springs.

Fig. 27 presents the *pdf* of the natural frequency spacings for one member from each of the four ensembles of the two plates coupled by linear springs. The *pdf*s are compared to a Rayleigh distribution calculated from

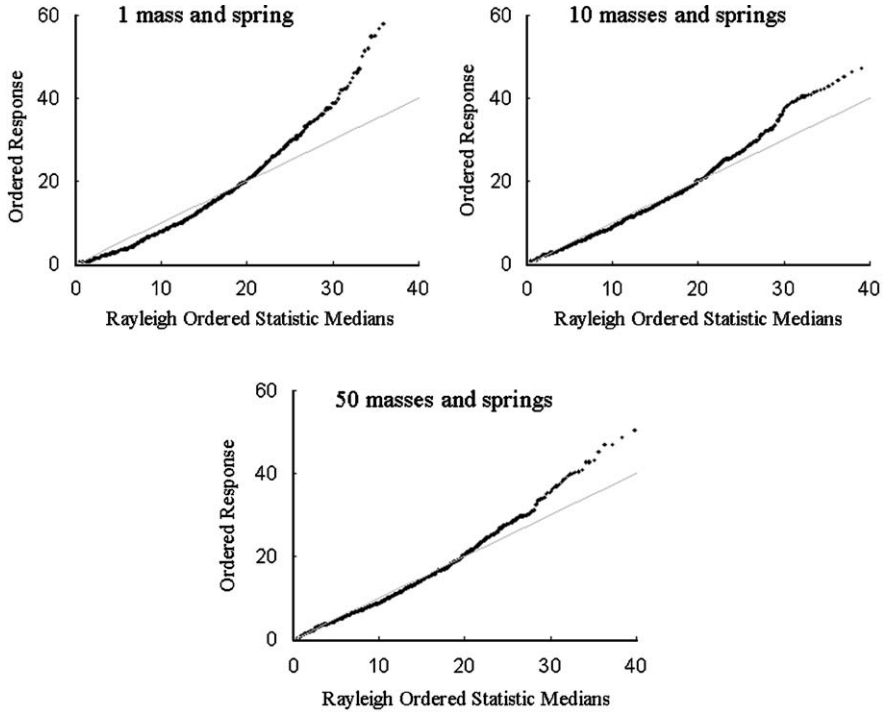

Fig. 24. Rayleigh probability plot of the ordered response (black points) and Rayleigh distribution line (grey line) of the frequency spacings for a plate with 1, 10 and 50 masses and linear springs to ground of different values and stiffness. Frequency range is 300 Hz to 12 kHz.

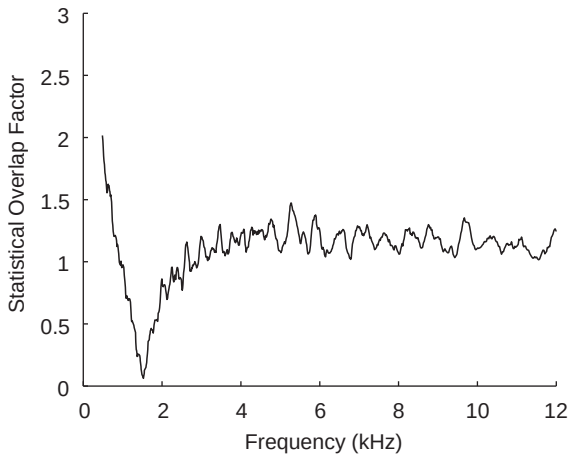

Fig. 25. Statistical overlap factor for a mass-and-spring-loaded plate. Results are presented for 50 collocated masses and linear springs to ground attached to the plate at random locations.

the mean frequency spacing for each ensemble corresponding to 7.1, 7.1, 7.3 and 7.5 Hz for 5, 10, 20 and 50 coupling springs. The mean frequency spacing does not significantly vary for the ensembles. Fig. 28 compares the Rayleigh probability plot of the ordered natural frequency spacings in the frequency range from 300 Hz to 5 kHz to a Rayleigh distribution line. Figs. 27 and 28 show that increasing the number of coupling springs results in a closer match to a Rayleigh distribution.

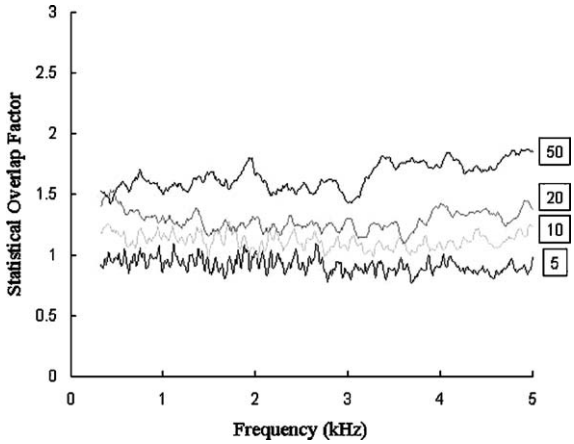

Fig. 26. Statistical overlap factor for two plates coupled by 5, 10, 20 and 50 linear springs of the same stiffness.

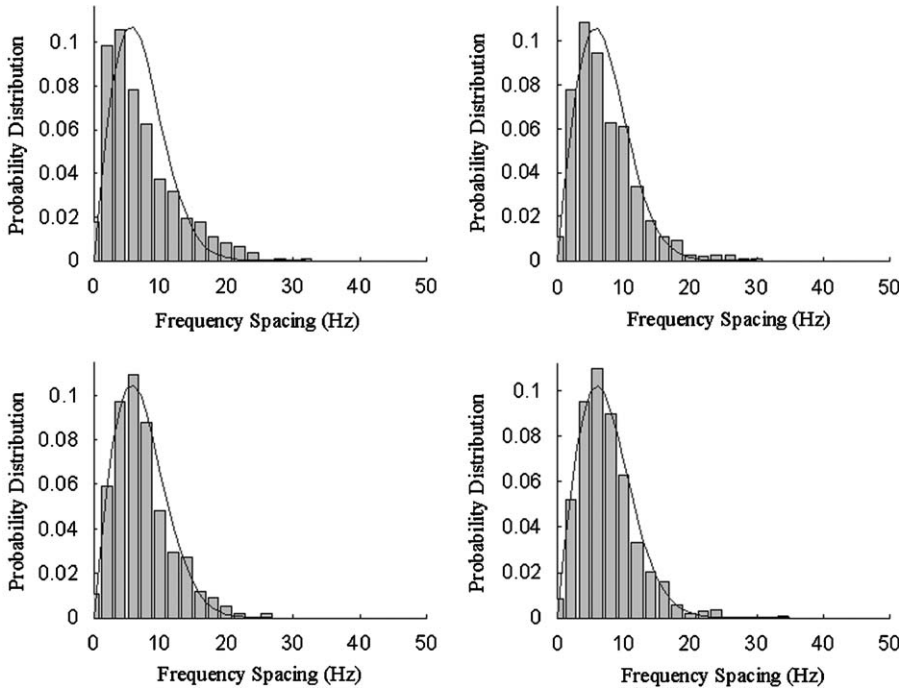

Fig. 27. Rayleigh distribution (black line) and *pdf* of the natural frequency spacings for two plates coupled by 5, 10, 20, and 50 springs of the same stiffness. Frequency range is 300 Hz to 5 kHz.

5.5. Plate with torsional edge springs

Simulation results are presented for an ensemble of rectangular steel plates to which torsional springs to ground were applied along the simply supported boundary edges of the plates. Fig. 29 presents the statistical overlap factors for ensembles consisting of 50 plates to which 10 torsional springs of stiffness 5 Nm/rad, 5 kNm/rad and 5 MNm/rad were randomly positioned along each edge. For low values of torsional spring stiffness ($K_t = 5$ Nm/rad), the value of the statistical overlap factor curves are nearly zero. The value of S increases as both the torsional stiffness and frequency increases. For each ensemble, the curves for S tend to level off. In Fig. 30, the *pdf*s of the natural frequency spacings for one member from each of the ensembles are compared to a Rayleigh distribution for a frequency range from 2 to 5 kHz. The corresponding mean

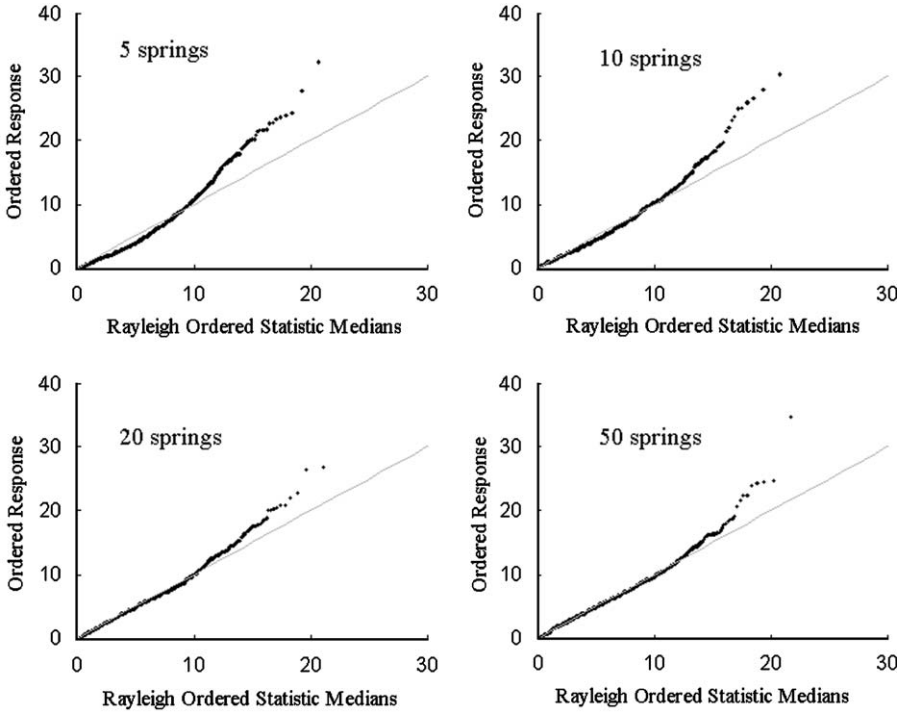

Fig. 28. Rayleigh probability plot of the ordered response (black points) and Rayleigh distribution line (grey line) of the frequency spacings for the two plates coupled by 5, 10, 20, and 50 springs of the same stiffness. Frequency range is 300 Hz to 5 kHz.

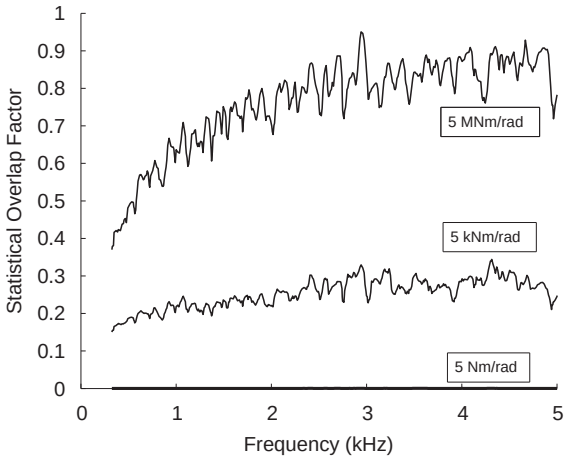

Fig. 29. Statistical overlap factor for a plate with torsional edge springs of stiffness 5 Nm/rad, 5 kNm/rad and 5 MNm/rad attached at random locations.

frequency spacings are 10.1, 10.2 and 10.3 Hz for the torsional springs of stiffness 5 Nm/rad, 5 kNm/rad and 5 MNm/rad, respectively. For a fixed number of torsional springs at the plate boundary edges, increasing the spring stiffness does not significantly affect the mean frequency spacing for the different ensembles. Fig. 31 compares the Rayleigh probability plot of the ordered natural frequency spacings to a Rayleigh distribution line. The results presented in Figs. 30 and 31 show that a Rayleigh distribution of the modal spacings is only achieved for high values of torsional spring stiffness (5 MNm/rad) and is attributed to the fact that the large torsional stiffness is effectively clamping the plates at the spring locations.

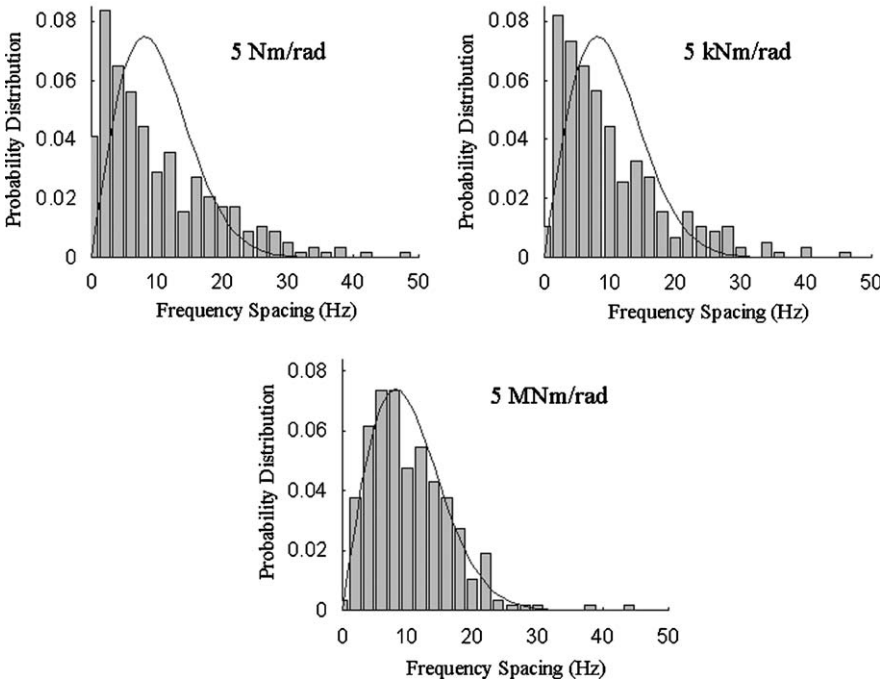

Fig. 30. Rayleigh distribution (black line) and *pdf* of the natural frequency spacings for a plate with torsional edge springs of stiffness 5 Nm/rad, 5 kNm/rad and 5 MNm/rad. Frequency range is 2–5 kHz.

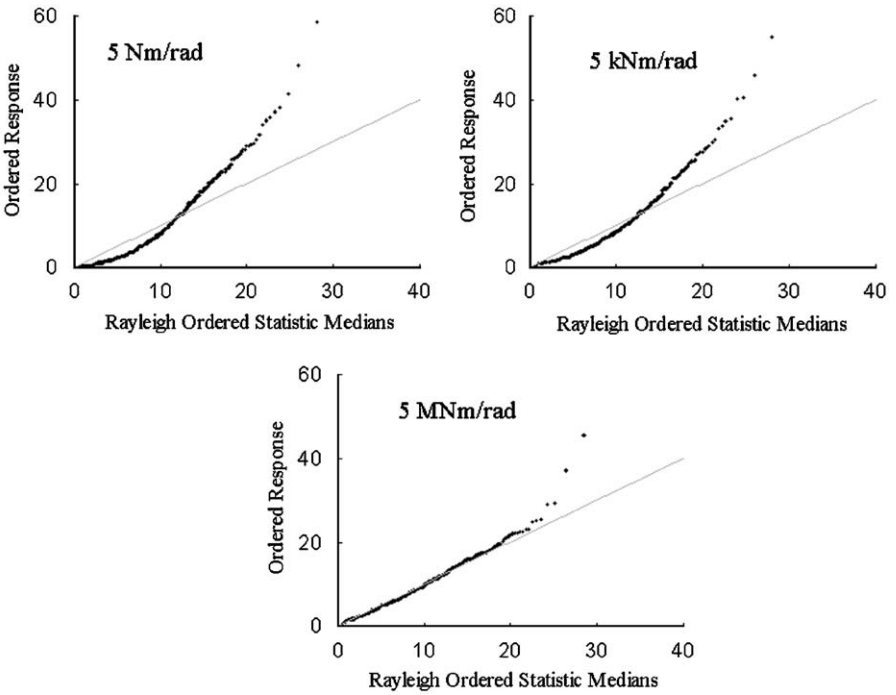

Fig. 31. Rayleigh probability plot of the ordered response (black points) and Rayleigh distribution line (grey line) of the frequency spacings for a plate with torsional edge springs of stiffness 5 Nm/rad, 5 kNm/rad and 5 MNm/rad. Frequency range is 2–5 kHz.

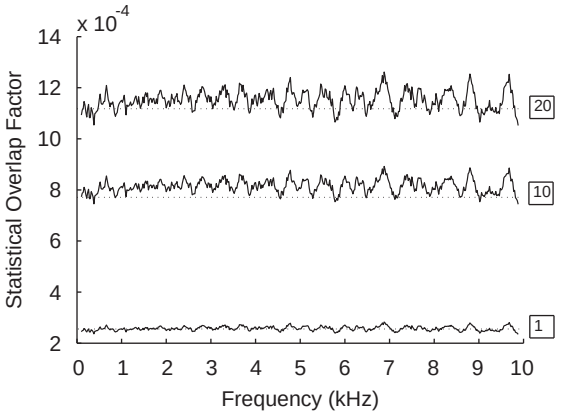

Fig. 32. Statistical overlap factor for a plate with torsional edge springs of stiffness 5 Nm/rad. The dotted lines represent the corresponding values for S from the perturbation analysis.

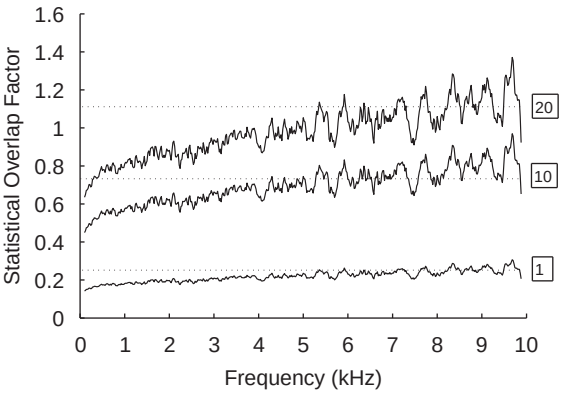

Fig. 33. Statistical overlap factor for a plate with torsional edge springs of stiffness 5 kNm/rad. The dotted lines represent the corresponding values for S from the perturbation analysis.

The statistical overlap factor was further investigated for the torsional edge spring plates with N_r number of torsional springs of stiffness K_t on each simply supported edge. Ensembles corresponding to 50 plates with 1, 10 and 20 added torsional springs to ground were generated by randomising the position of the springs, for a low value of torsional spring stiffness (5 Nm/rad) and higher value (5 kNm/rad). For the various K_t, N_r combinations, the mean natural frequencies, their standard deviation and the mean frequency spacing across the ensemble were calculated from the eigenvalue analysis of Eq. (14). Using Eq. (15), the statistical overlap factor of the plate ensembles for the different K_t, N_r combinations were obtained and the trendline curves are presented in Fig. 32 ($K_t = 5$ Nm/rad) and Fig. 33 ($K_t = 5$ kNm/rad). Using the ensemble mean frequency spacing for a given K_t, N_r combination, the values from the approximate expression developed for S given by Eq. (38) are also shown in Figs. 32 and 33 as dotted lines. Fig. 32 shows that for low values of torsional spring stiffness (5 Nm/rad), the statistical overlap factor curves are nearly constant with frequency. Very good agreement between the statistical overlap curves for the plate ensembles with edge springs of 5 Nm/rad and the values for S obtained by the perturbation analysis can also be observed. Fig. 33 shows that the statistical overlap factor tends to increase as both the value of K_t and number of added springs increase. For large values of K_t, the springs will act has a clamp and the perturbation analysis is no longer valid. In addition, for large numbers of added springs, the springs are separated by less than half a wavelength for which the perturbation analysis is not valid.

6. Conclusions

Engineering structures are complex in geometry and generally possess variability in their material or geometric properties. This work investigates the extent to which Gaussian orthogonal ensemble (GOE) statistics is applicable to the natural frequencies of practical engineering structures. A range of structural uncertainties were investigated corresponding to uncertainty due to mass and stiffness perturbations, uncertainty at the boundaries of a structure and uncertainty in the coupling between the subsystems of a structure. For each structure, the effect of the different types of uncertainty and the degrees of uncertainty on the natural frequency statistics has been investigated in detail. Based on a first-order perturbation analysis, an approximate expression for the statistical overlap factor has been developed for mass and spring loaded plates.

A summary on the major findings for the natural frequency statistics are as follows:

- Stiffness perturbation due to the addition of linear springs to ground was found to affect the lowest frequency modes of a dynamic system. As the frequency increased, the effect of stiffness perturbations on variation in the natural frequencies dramatically decreased.
- Mass perturbations were shown to affect the mid and high frequency modes of a structure. The variation in the natural frequencies increased as the frequency increased, which is attributed to the inertia of the masses becoming more significant. Variation in the natural frequencies also increased for a greater degree of uncertainty, generated by either increasing the size of the added masses or the number of added masses.
- Increasing the number of added masses tended to have a greater effect on the variation in the natural frequencies compared to increasing the size of the added masses. This is attributed to the fact that increasing the number of masses results in greater deformation of the physical symmetry of a structure.
- For a given structure with uncertainty, it was observed that there is a frequency beyond which the structure has saturated with uncertainty, such that any further increase in frequency or degree of uncertainty does not affect the variation of the natural frequencies.
- For a sufficient amount of structural uncertainty, the modal spacings of a structure tend to a Rayleigh distribution, which indicates universality of the modal statistics regardless of the type of uncertainty.

Acknowledgement

The author would like to acknowledge Prof. R.S. Langley, Cambridge University, for his contribution of ideas to the work described in this paper.

References

[1] M.S. Kompella, B.J. Bernhard, Variation of structural-acoustic characteristics of automotive vehicles, *Noise Control Engineering Journal* 44 (1996) 93–99.
[2] C. Soize, Random matrix theory and non-parametric model of random uncertainties in vibration analysis, *Journal of Sound and Vibration* 263 (2003) 893–916.
[3] R.S. Langley, V. Cotoni, Response variance prediction in the statistical energy analysis of built-up systems, *Journal of the Acoustical Society of America* 115 (2004) 706–718.
[4] R.H. Lyon, Statistical analysis of power injection and response in structures and rooms, *Journal of the Acoustical Society of America* 45 (1969) 545–565.
[5] M.L. Mehta, *Random Matrices*, Academic Press, New York, 1991.
[6] R.L. Weaver, Spectral statistics in elastodynamics, *Journal of the Acoustical Society of America* 85 (1989) 1005–1013.
[7] P. Bertelsen, C. Ellegaard, E. Hugues, Distribution of eigenfrequencies for vibrating plates, *European Physical Journal B* 15 (2000) 87–96.
[8] R.S. Langley, A.W.M. Brown, The ensemble statistics of the band averaged energy of a random system, *Journal of Sound and Vibration* 275 (2004) 823–846.
[9] A.W.M. Brown, The Ensemble Statistics of the Response of Structural Components with Uncertain Properties, PhD Thesis, University of Cambridge, UK, 2003.
[10] R.S. Langley, Mid and high-frequency vibration analysis of structures with uncertain properties, *Proceedings of the Eleventh International Congress on Sound and Vibration*, St. Petersburg, Russia, 5–8 July 2004.

[11] C.S. Manohar, A.J. Keane, Statistics of energy flows in spring-coupled one-dimensional subsystems, *Philosophical Transactions of the Royal Society A: Physical and Engineering Sciences* 346 (1994) 525–542.
[12] L. Meirovitch, *Elements of Vibration Analysis*, second ed., McGraw Hill, New York, 1986.
[13] N.J. Kessissoglou, R.S. Langley, Application of the statistical overlap factor to predict GOE statistics, *Proceedings of NOVEM 2005*, St. Raphaël, France, 18–21 April 2005.
[14] R.S. Langley, SEA: current and future research needs, *Proceedings of the First International AutoSEA Users Conference*, San Diego, USA, 27–28 July 2000.
[15] R.H. Lyon, R.G. DeJong, *Theory and Application of Statistical Energy Analysis*, second ed., Butterworth Heinemann, Oxford, 1995.
[16] J.M. Chambers, W.S. Cleveland, B. Kleiner, P.A. Tukey, *Graphical Methods for Data Analysis*, Duxbury Press, Boston, MA, USA, 1983.
[17] A. Papoulis, *Probability, Random Variables, and Stochastic Processes*, second ed., McGraw-Hill, New York, 1984.